Depositional history, tectonics, and detrital zircon geochronology of Ordovician and Devonian strata in southwestern Mongolia

T.M. Gibson[1], P.M. Myrow[1,†], F.A. Macdonald[2], C. Minjin[3], and G.E. Gehrels[4]

[1]*Department of Geology, Colorado College, 14 E. Cache La Poudre Street, Colorado Springs, Colorado 80903, USA*

[2]*Department of Earth and Planetary Sciences, Harvard University, Oxford Street, Cambridge, Massachusetts 02138, USA*

[3]*Research Center for Stratigraphy and Paleontology, School of Geology and Petroleum Engineering, Mongolian University of Science and Technology, Ulaanbaatar-46, Mongolia*

[4]*Department of Geosciences, University of Arizona, Tucson, Arizona 85721, USA*

ABSTRACT

Lower Paleozoic successions of the Gobi-Altai zone of southern Mongolia record an abrupt facies transition from deposition of predominantly fine-grained uppermost Ordovician through lowermost Devonian carbonate and marl facies to deposition of coarse clastic strata of the Lower Devonian Tsakhir Formation. The Tsakhir generally fines upward from alluvial-fan cobble and pebble conglomerate to interbedded coarse- and fine-grained marine siliciclastic and carbonate strata, which were deposited within a tectonically active basin. The marine strata, deposited in a storm-influenced proximal to distal fan delta, include unusual event beds that grade from pebble conglomerate to hummocky cross-stratified grainstone and sandstone. These beds represent sediment emplaced by gravity flows during flood events and reworked by large gravity waves associated with storm events. The interpreted link between flood deposition and storm wave reworking supports a hyperpycnal flow interpretation for these deposits.

The sudden facies transition at the base of the formation represents the sedimentological and stratigraphic signature of Early Devonian tectonism in the Gobi-Altai zone. The general upward-fining pattern of the Tsakhir is interpreted as a response to the creation of accommodation space at a greater rate than progradation of the fan delta, in large part due to tectonic subsidence, although some component of eustasy may have been involved. The production of steep relief and deposition of associated volcanics suggest a transition from relatively passive deposition to active tectonics in this region during the Lochkovian to Pragian stages of the Early Devonian. We herein introduce the term "Tsakhir event" for this important tectonic transition. Range-bounding faults for this event are not preserved, but alluvial-fan deposition, the development of unconformities, renewed subsidence, and magmatism throughout the Gobi-Altai zone all suggest syndepositional tectonism.

Detrital zircon spectra from both Ordovician and Devonian strata contain Archean to Paleozoic ages. Minor differences between Ordovician and Devonian samples suggest changes in source regions and/or transport paths prior to, and after, the Tsakhir event. The paleoenvironmental setting of the Tsakhir Formation requires short transport distances, and thus the age spectrum of a sample from this formation represents proximal basement rocks of the Shine Jinst region of the Gobi-Altai zone. Basement rocks are not exposed in the Shine Jinst region, but the wide variety of ages in all of the detrital spectra suggest a nearby continental source.

Our detrital age spectra contain peaks that coincide with basement ages and magmatic events on the adjacent Mongolian microcontinent and also have strong similarities with recently published spectra of nearby landmasses in Neoproterozoic to Paleozoic paleogeographic reconstructions, namely, Siberia, North China, eastern Gondwana, and Tarim. These similarities extend to spectra of late Neoproterozoic to middle Paleozoic rocks throughout Gondwanaland and also Siberia, illustrating the somewhat limited utility of detrital spectra for determining the tectonic affinities of crustal blocks at this time in Earth history.

INTRODUCTION

Southern Mongolia is centrally located within the Central Asian orogenic belt, a Neoproterozoic to early Mesozoic accretionary zone that juxtaposed microcontinents and island arcs between Baltica, Siberia, Tarim, and North China (Şengör et al., 1993; Zorin et al., 1993; Lamb and Badarch, 1997; Heubeck, 2001; Badarch et al., 2002; Wang et al., 2005; Briggs et al., 2007; Windley et al., 2007; Kelty et al., 2008; Kröner et al., 2010). The Central Asian orogenic belt is the largest area of Phanerozoic crustal growth on Earth (Şengör et al., 1993), but the timing and nature of the orogenic events remain poorly constrained. This is due in part to the paucity of studies on temporally constrained syntectonic strata in southern Mongolia, and also due to post-Paleozoic tectonic complications. Detailed sedimentological data combined with chronostratigraphically constrained geochronological data are needed in order to reconstruct the tectonic history of this region and decipher regional relationships with adjacent tectonic blocks.

In this paper, we provide the first detailed sedimentological and stratigraphic study of the Lower Devonian Tsakhir Formation in the Shine Jinst region of southern Mongolia (Fig. 1). This unit records a stratigraphic transition from underlying Upper Ordovician to lowermost Devonian quiet water carbonate deposits to coarse conglomerate, sandstone, and siltstone of the Tsakhir, which has been interpreted to record uplift and erosion of these older carbonate units (Lamb and Badarch, 1997). Our sedimentological analyses, in combination with detrital zircon geochronology data for a suite of chronostratigraphically constrained samples that span this tectonic transition, provide important insights into the depositional history and the tectonic evolution of the Gobi-Altai zone, and more generally, the Central Asian orogenic belt.

GEOLOGICAL SETTING AND STUDY LOCATION

Shine Jinst is located in the Gobi-Altai zone of southern Mongolia, directly south of the Main Mongolian Lineament (Fig. 1), which separates

†E-mail: pmyrow@ColoradoCollege.edu

GSA Bulletin; May/June 2013; v. 125; no. 5/6; p. 877–893; doi: 10.1130/B30746.1; 12 figures; Data Repository item 2013145.

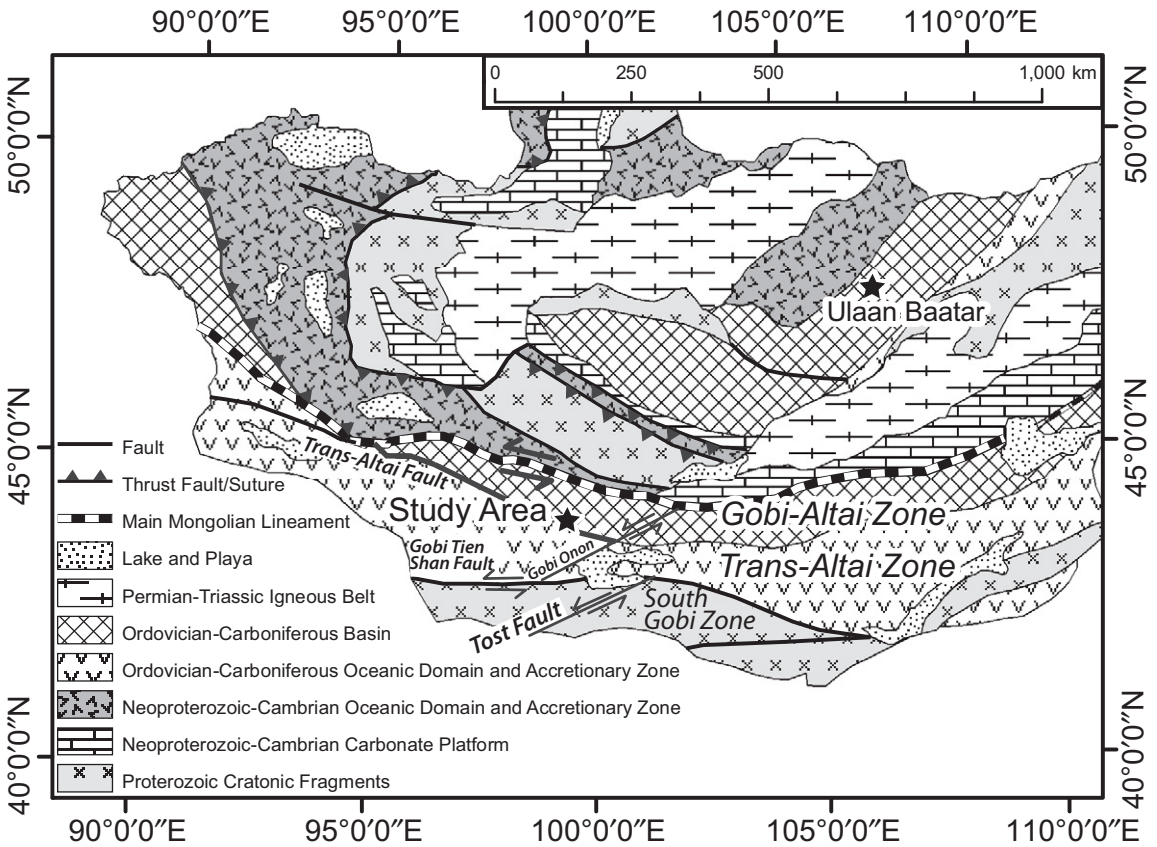

Figure 1. Tectonic map of Mongolia modified from Macdonald et al. (2009) and Kröner et al. (2010) with location of study area indicated. The Mandalovoo subzone is the southern part of the Gobi-Altai zone.

Neoproterozoic to early Paleozoic continental fragments, arcs, and accretionary zones to the north from Ordovician to Carboniferous terranes to the south (Kröner et al., 2010). The southern margin of the Gobi-Altai zone is defined by the Trans-Altai fault (Fig. 1), which is in contact with the Paleozoic oceanic domain of the Trans-Altai zone (Zorin et al., 1993; Kröner et al., 2010). The Trans-Altai zone was an active accretionary arc system through the end of the Paleozoic (Lamb and Badarch, 1997), when the closure of the paleo–Asian Ocean culminated in the collision of northern China and southern Mongolia (Johnson et al., 2008; W. Xiao et al., 2008, 2010; W.J. Xiao et al., 2009b; Chen et al., 2010). During the Mesozoic, the tectonic and sedimentary setting changed from a convergent margin to an intracontinental setting with sinistral transpression (M.A. Lamb et al., 2008). During the Jurassic, a major left-lateral strike-slip system developed in Asia, which included the Tost and Gobi Onon faults in southern Mongolia (Fig. 1). These faults have the same orientation and sense of motion as left-lateral faults and associated wrench thrust faults in the Shine Jinst region (Fig. 2; M.A. Lamb et al., 2008). Intracontinental deformation continued through the Cenozoic and is responsible for sinistral displacement and reactivation of the east-west–oriented Main Mongolian Lineament and Gobi Tien Shan fault (Fig. 1; M.A. Lamb et al., 2008; Briggs et al., 2009; Cunningham, 2010).

The oldest strata exposed in the Shine Jinst region consist of biostratigraphically constrained Upper Ordovician to lowermost Devonian carbonate rocks with minor sandstone, shale, and conglomerate (Wang et al., 2005). The Lower Devonian Tsakhir Formation unconformably overlies these carbonate rocks and records a sharp stratigraphic contact due to uplift and erosion of the older carbonate strata (Lamb and Badarch, 1997). QFL ternary plots demonstrate that Devonian sandstone samples near Shine Jinst are richer in lithics than underlying Silurian and Ordovician strata, and they suggest a volcanic arc source (Lamb and Badarch, 2001). The base of the Tsakhir consists of cobble conglomerate dominated by limestone clasts that were sourced from the underlying units. The section fines upward to interbedded conglomerate and sandstone, and then to interbedded sandstone, grainstone, siltstone, and mudstone. Felsic volcanic deposits also exist in the upper half of the unit. The formation has been generally interpreted to represent braided fluvial or fan-delta to shallow-marine deposits (Lamb and Badarch, 1997).

The Tsakhir Formation is exposed in multiple fault blocks near the Huvchuu well in the Shine Jinst region of the Gobi-Altai zone in southern Mongolia (Fig. 2). The base of the measured section described here is at 44°21′38.4″N and 99°26′47.0″E at 1890 m elevation. The Huvchuu well in Shine Jinst is accessed via a long drive (~900 km) southwest from Ulaanbaatar on poorly maintained, rural tracks.

STRATIGRAPHY

The Tsakhir Formation unconformably overlies different stratigraphic levels of the uppermost Silurian to lowermost Devonian (Pridolian-Lockhovian) Amansair Formation. The Amansair Formation is 30 m to 40 m thick and contains a lower fossiliferous carbonate member and an upper reddish-gray to greenish-gray siltstone and sandstone member with felsic volcanic deposits. The Tsakhir Formation is

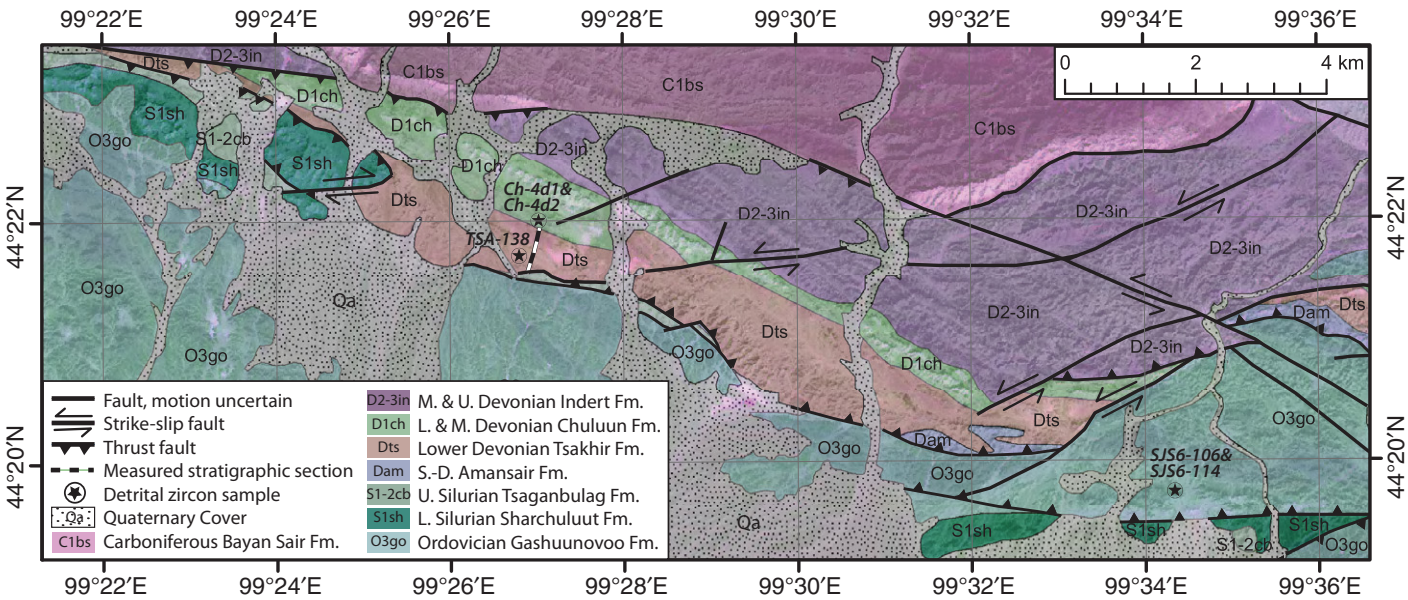

Figure 2. Geological map of the Shine Jinst area draped on a LandSat image. Geology is modified from Minjin (2001) and M.A. Lamb et al. (2008).

conformably overlain by the Lower Devonian (Pragian to Emsian) Chuluun Formation (Fig. 3; Wang et al., 2005), which consists of 480 m of dark-gray, thin-bedded, fossiliferous, flaggy and biohermal limestone; dark-green calcareous and noncalcareous argillite; siltstone to coarse sandstone; and fine to coarse clastic tuff. Conodonts from the Tsakhir Formation, in conjunction with those found in strata both above and below the Tsakhir, indicate a Lower Devonian (Lochkovian-Pragian) age (Wang et al., 2005).

The Tsakhir Formation at Shine Jinst contains faults with apparent displacements of up to 10 m, but marker beds were used to correlate across these faults in nearly all cases. The formation is 630 m thick and records upward fining from cobble and pebble conglomerate to finer-grained siliciclastic and carbonate lithologies. The base of the Tsakhir Formation at Shine Jinst is in fault contact with the uppermost Silurian to lowermost Devonian Amansair Formation with very low-angle truncation. Evidence for marine deposition exists at numerous stratigraphic levels in the Tsakhir Formation, including bryozoan and rugose coral fossils in a grainstone bed at 115 m, a stromatoporoid bed at 382 m, and locally abundant bioturbation high in the section.

LITHOFACIES

We measured 630 m of section at a centimeter to meter scale through the Tsakhir Formation in the Shine Jinst region, including several volcanic units (Fig. 4). Six lithofacies are defined and described next.

Conglomerate Facies

This facies consists of massive, very poorly sorted, rounded to subrounded, clast-supported, conglomerate beds. The basal 90 m section of the formation is composed of massive to very crudely bedded cobble to boulder conglomerate. This basal unit lacks interbedded finer-grained facies and shows no obvious imbrication. Above this, conglomerate beds of similar grain size are a few tens of centimeters to 4 m thick, and they decrease in abundance up section. A few thicker beds (5.6 m to 9.6 m) of coarse conglomerate exist in association with volcanic units between 400 m and 500 m in the section (Fig. 5). Most of the cobble conglomerate beds are massive, with no obvious grading. Clasts in these cobble conglomerate beds reach a maximum diameter of ~35 cm. Pebble conglomerate beds are also present throughout the section, and they generally decrease in bed thickness and abundance stratigraphically up section. Clasts average 2 cm in diameter, although outsized clasts reach 30 cm in diameter. Many beds of both the coarse and fine conglomerate have erosional bases, and in places are lenticular (Fig. 6). Some beds contain intraclasts of similar composition to the underlying beds.

The clasts consist of grainstone, wackestone, skeletal wackestone, graywacke, calcareous sandstone, silty skeletal wackestone, carbonate mudstone, dolostone, and large bioclasts of tabulate coral and stromatoporoids. In most beds, the clasts have been structurally stretched along cleavage planes, which are generally subparallel to bedding. Some clasts contain parallel sets of quartz- and calcite-filled fractures that do not extend beyond clast boundaries and have variable orientations (Fig. 7), whereas others penetrate both clasts and matrix (Fig. 7). The matrix commonly weathers brown and consists of very coarse-grained, calcareous, lithic and quartz sandstone with many granules. It is composed of 40%–80% quartz grains that range from coarse sand to granule in size. The lithic grains are dominantly carbonate.

Calcareous Sublitharenite Facies

Gray, well-sorted, subangular to subrounded, thinly bedded, fine- to coarse-grained sublitharenite with calcareous cement is present throughout much of the formation. Beds range from 1 cm to 50 cm in thickness, with most between 2 cm and 5 cm. Quartz grains make up 70% of this facies, and lithic fragments and calcite grains comprise the remaining 30%. Clasts composed of dark-gray micrite up to 2 cm in diameter are also sporadically present in this facies. Many beds exhibit hummocky cross-stratification and symmetrical ripples (Fig. 8), and where both are present, the latter rests above the former. Beds exhibiting hummocky cross-stratification range from 3 cm to 40 cm thick, and spacings between hummocks range from tens of centimeters to a few meters in scale.

Sandy Grainstone Facies

This facies is composed of poorly sorted, well- to subrounded, fine- to very coarse-grained, sandy grainstone. Bed thicknesses range from

1 cm to 35 cm, and most are between 2 cm and 5 cm. Quartz content ranges from 5% to 40%, and lithic fragments make up less than 5%. Pebble-rich grainstone beds of this facies represent transitional facies with the pebble conglomerate described above (Fig. 8). These beds contain sandstone and micrite clasts up to 9 cm in diameter. Some beds fine upward from pebble-bearing grainstone to finer-grained grainstone with hummocky cross-stratification and ripple-scale cross-bedding. Locally, starved ripples occur in the uppermost parts of beds of this facies at transitions to finer-grained overlying strata.

Very Fine- to Fine-Grained Grainstone Facies

Very fine- to fine-grained, well-sorted, blue-green weathering grainstone facies make up beds that range from 2 mm to 40 cm thick. The grainstone has 1–4-mm-thick fissile breaks that result in a distinctive paper-thin weathering pattern. It consists of 15%–25% quartz grains, and some beds contain a minor percentage of floating medium to coarse quartz sand and pebbles. Parallel lamination is present within some beds of this facies. Bedding-plane–parallel burrows are conspicuous in beds of this facies between 370 m and 400 m in the section. This facies is abundant lower in the formation and becomes less abundant, more thinly bedded, and finer grained above 400 m.

Calcareous Siltstone Facies

This facies is composed of red, calcareous siltstone with lenses of marly carbonate concretions, and it is solely present above 500 m in the formation. Beds of this facies tend to be highly cleaved and laterally discontinuous, and range from tens of centimeters to tens of meters in thickness. Abundant dark-purple clay-lined burrows that average 7 mm in diameter exist along bedding planes (Fig. 9).

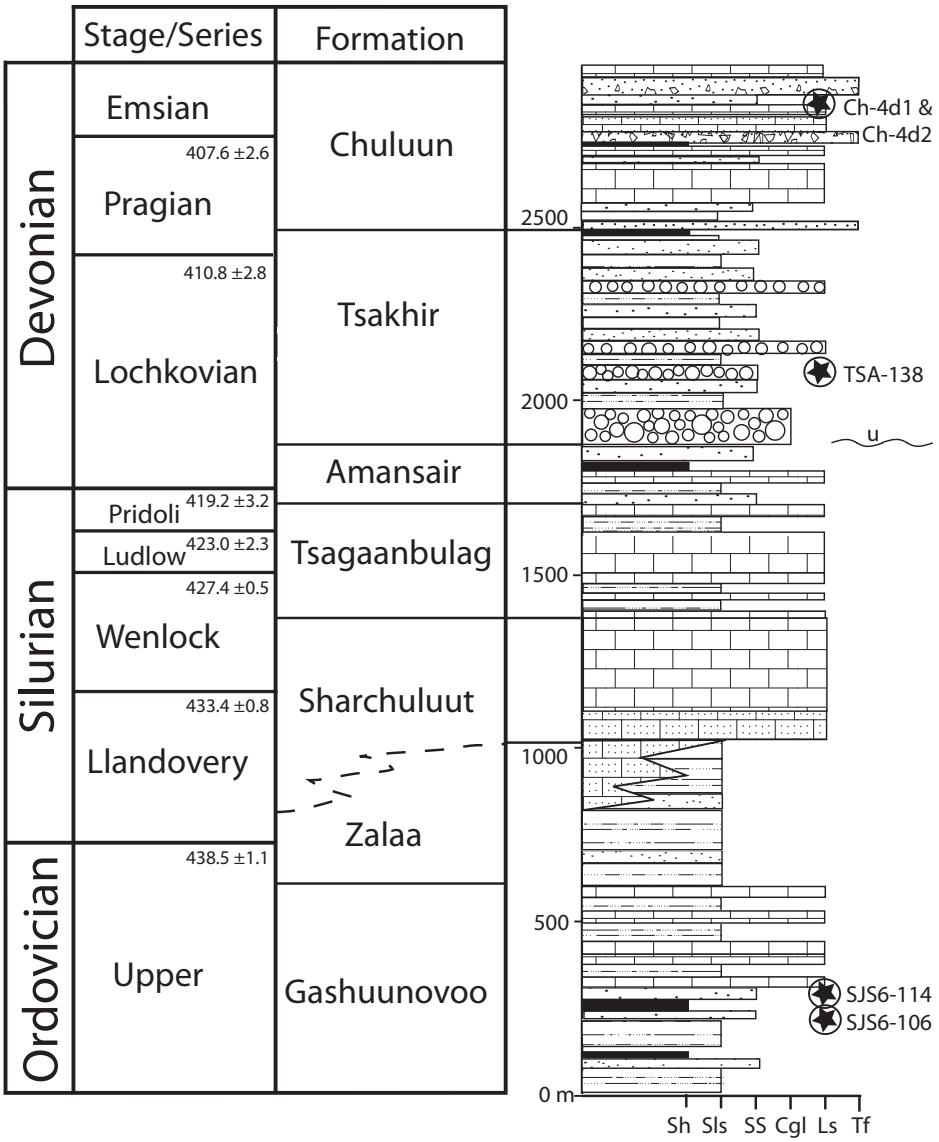

Figure 3. Stratigraphy of the Shine Jinst region of southern Mongolia with stratigraphic heights of detrital zircon samples. Sh—shale, Sls—siltstone, SS—sandstone, Cgl—conglomerate, Ls—limestone/sandy limestone, Tf—tuff, and u—unconformity.

Upward-Fining Beds

The Tsakhir Formation contains many 50-cm- to 3-m-thick upward-fining beds. Many of these beds contain a lower division of clast-supported and ungraded pebble conglomerate 5 cm to 75 cm thick. These commonly exhibit scoured bases, and in cases, channel geometries. These beds grade into pebble-bearing sandy divisions of either grainstone or sublitharenite. Many of these upward-fining beds lack conglomeratic basal divisions and instead have sandy divisions at the base. The finer sandy facies are generally 10 cm to 150 cm thick. They commonly drape underlying conglomerate and exhibit parallel lamination, hummocky cross-stratification, and trough cross-bedding (Figs. 8 and 10–11). In nearly all beds, very fine grainstone or calcareous siltstone, 10 cm to 4.15 m thick, rests above the sandy facies. In one bed, fine sandstone with hummocky cross-stratification is overlain by calcareous siltstone that contains fine sandstone starved ripples.

Volcanic Facies

Massive, green, rhyolitic-tuff beds and volcanic flow deposits are present above ~400 m in the formation. These grade into fine- to coarse-grained volcaniclastic sandstone in places. The pure tuff beds are green and glassy in texture. The flows generally have porphyritic-aphanitic textures and are composed of quartz, plagioclase, and clays. Most of the volcanic units have been recrystallized, and minimal original texture is preserved. Phenocrysts include resorbed quartz and plagioclase, and the groundmass is fine grained and felted. The ancillary minerals include apatite, zircon, and muscovite (sericite). Bed thicknesses vary from 5 m to 35 m.

LITHOFACIES INTERPRETATIONS

The basal conglomerate rests unconformably on predominantly fine-grained Ordovician through lowermost Devonian limestone and

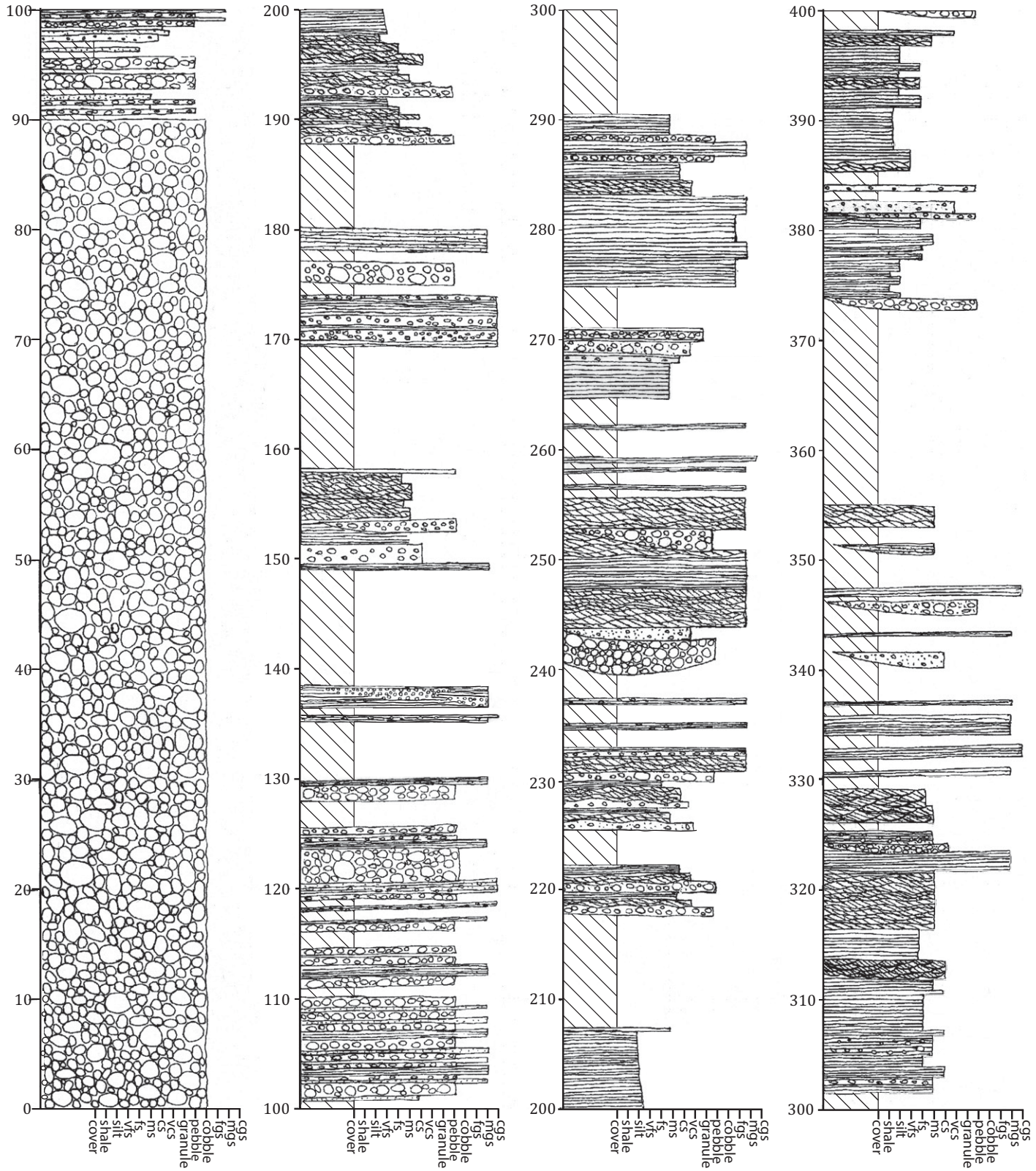

Figure 4 (*on this and following page*)**. Detailed stratigraphic section (0–630 m) of Tsakhir Formation in the Shine Jinst region. The calcareous sublitharenite facies is plotted as the appropriate grain size of sandstone (fine [fs], medium [ms], coarse [cs], very coarse [vcs]), the calcareous siltstone is plotted as siltstone (silt), and the two grainstone facies are plotted as the appropriate grain size of grainstone (fgs, mgs, cgs).**

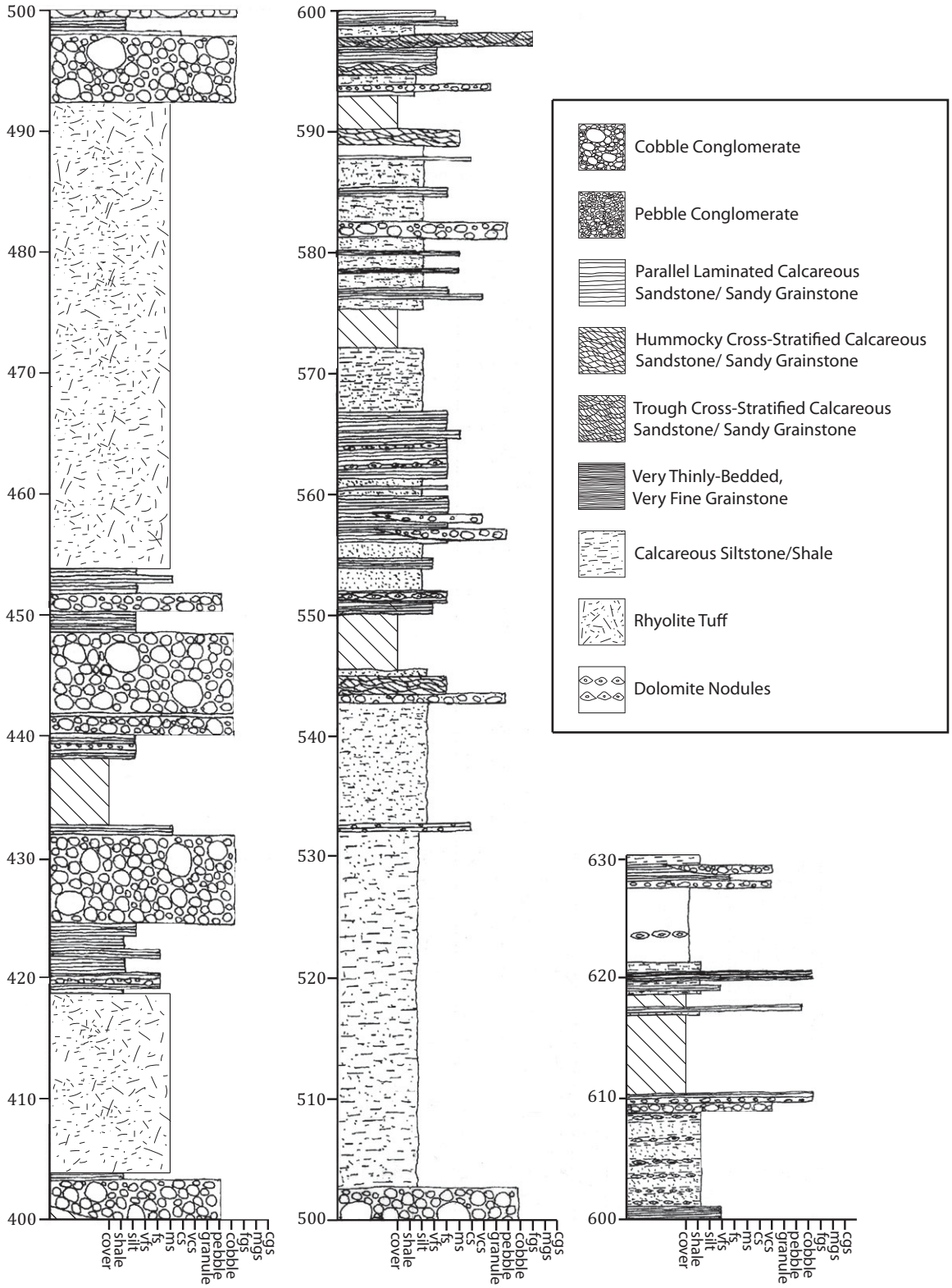

Figure 4 (*continued*).

Figure 5. Thick volcanic (V) and conglomerate (C) succession in the foreground at 404 m to 492 m stratigraphic height. These rocks are on strike with Emsian limestone outcrop (Em) in the background due to faulting. Dark volcanic unit in foreground is 38 m thick.

marl deposits and represents a sharp facies transition to carbonate cobble conglomerate with abundant siliciclastic sand and silt matrix. The transition requires uplift and erosion of both underlying carbonate strata and basement rock that contains quartz. Large clast sizes, and a similarity in composition of clasts to the underlying carbonate units suggest that faulting and exposure of these strata provided a local source for the conglomerate (Lamb and Badarch, 1997). The presence of clasts with fracture fills suggests structural deformation of the source material prior to erosion and deposition. The thickness (90 m) and coarse nature of the basal conglomerate reflect deposition on steep slopes and short transport distances of a proximal subaerial setting. The lack of interbedded finer-grained facies and obvious imbrication, as well as a predominance of massive bedding, suggests deposition from high-viscosity flows, i.e., debris flows (Major, 1997).

The large size and moderate rounding of limestone clasts imply a proximal source that was dominated by mass movement events and potentially high-concentration streamfloods along steep gradients (Daily et al., 1980; Kim et al., 1995; Jo et al., 1997). We interpret the basal 90-m-thick conglomerate unit as a subaerial deposit of a debris-flow– and streamflood-dominated coastal alluvial fan in a tectonically active basin directly adjacent to a steep catchment basin (e.g., M.P. Lamb et al., 2008; Myrow et al., 2008).

The abundance of coarse- to very coarse-grained quartz sand grains in the matrix of this facies and the paucity of quartz-bearing clasts are enigmatic. Sandstone deposits exist in the underlying formations, but they make up a minor volume of the rock, and thus it is unlikely that they could have supplied all of the quartz sand found throughout the Tsakhir Formation. The quartz sand was likely derived from erosion of local basement, although erosion of unknown poorly lithified pre-Ordovician sandstone-rich deposits could also have been a source of such quartz sand. For conglomerate and sandstone beds higher in the section, interpreted as marine facies, it is possible that a separate source of coarse quartz grains may have existed in shoreline environments that could have been mobilized and mixed with the larger clasts during emplacement.

The transition into predominantly interbedded pebble conglomerate; medium- to coarse-grained calcareous sublitharenite; fine- to very coarse-grained sandy grainstone; and very fine-grained grainstone above 90 m is interpreted as a flooding surface and subsequent deposition in a shallow-marine setting. This is supported by the presence of fossiliferous beds with bryozoa, rugosa, and stromatoporoids, as well as bioturbated beds higher in the section.

The channel-form conglomerate beds in these marine deposits have erosional lower boundaries and intraclasts of underlying fine-grained lithologies, which reflect initial erosion under turbulent flows. The depositional phase of the events that emplaced these beds was likely characterized by very high-concentration flows, given the near absence of grading within the conglomerate beds. The calcareous sublitharenite and sandy grainstone facies show evidence for traction deposition under the influence of waning flow, including the variety of stratification types and sequences described previously herein (e.g., hummocky cross-stratification overlain by ripple cross-stratification), as well as graded bedding. Parallel lamination, hummocky cross-stratification, symmetrical and asymmetrical ripples, and ripple-scale cross-lamination reflect traction transport and deposition under flows of variable intensity. The presence of hummocky cross-stratification and symmetrical ripples in event beds suggests deposition within a storm- and wave-influenced shallow-marine setting (Myrow and Southard, 1996). Detailed sedimentological analyses of these beds and the possible modes of emplacement are provided later herein.

The interbedding of these sandy facies with the very fine grainstone and calcareous siltstone facies reflects alternation of event bed and suspension deposition, the latter of which represents background deposition between events. Such alternation requires deposition below fair-weather wave base, an interpretation supported by a complete lack of features that record subaerial exposure. Beds with pebble conglomerate and pebbly sandstone divisions at their base, and hummocky cross-stratification sandstone divisions above, are also interbedded with finer material that is interpreted as background marine deposition, and thus also require that deposition took place offshore.

Some of these fine-grained facies that directly overlie event beds may have also been deposited during the waning stages of storm currents that deposited the conglomeratic and sandy facies, as opposed to background deposition between storm events. Some of these deposits may also represent suspension deposition from buoyant plumes (hypopycnal flows) that also formed from floods entering the basin from adjacent alluvial fans.

The red calcareous siltstone of the upper part of the formation reflects increased oxidation of iron phases in the sediment, suggesting that the upper sediment column and/or bottom waters of the basin became better oxygenated relative to the lower part of the section. This is supported by the presence of thick bioturbated beds only in the upper part of the formation. The general paucity of fossils and bioturbation lower in the section may be a result of high rates of sediment input and/or generally unfavorable bottom water chemistry, such as lower oxygen levels.

The volcanic facies represent flows and tuffs that were deposited in shallow-marine environments, and possibly altered in part through contact with marine water. Coarse volcaniclastic sandstone formed by reworking of volcanic material with terrestrial sediment. The volcanic material could represent a combination of sediment directly deposited in the ocean from air-fall and terrestrial volcanic sediment that was delivered to the ocean by fluvial transport. Fine-grained, glassy, rhyolitic tuff beds were deposited as air fall into standing water (Stratford and Aitchison, 1996).

Given the evidence for tectonic activity described here, the general upward-fining trend

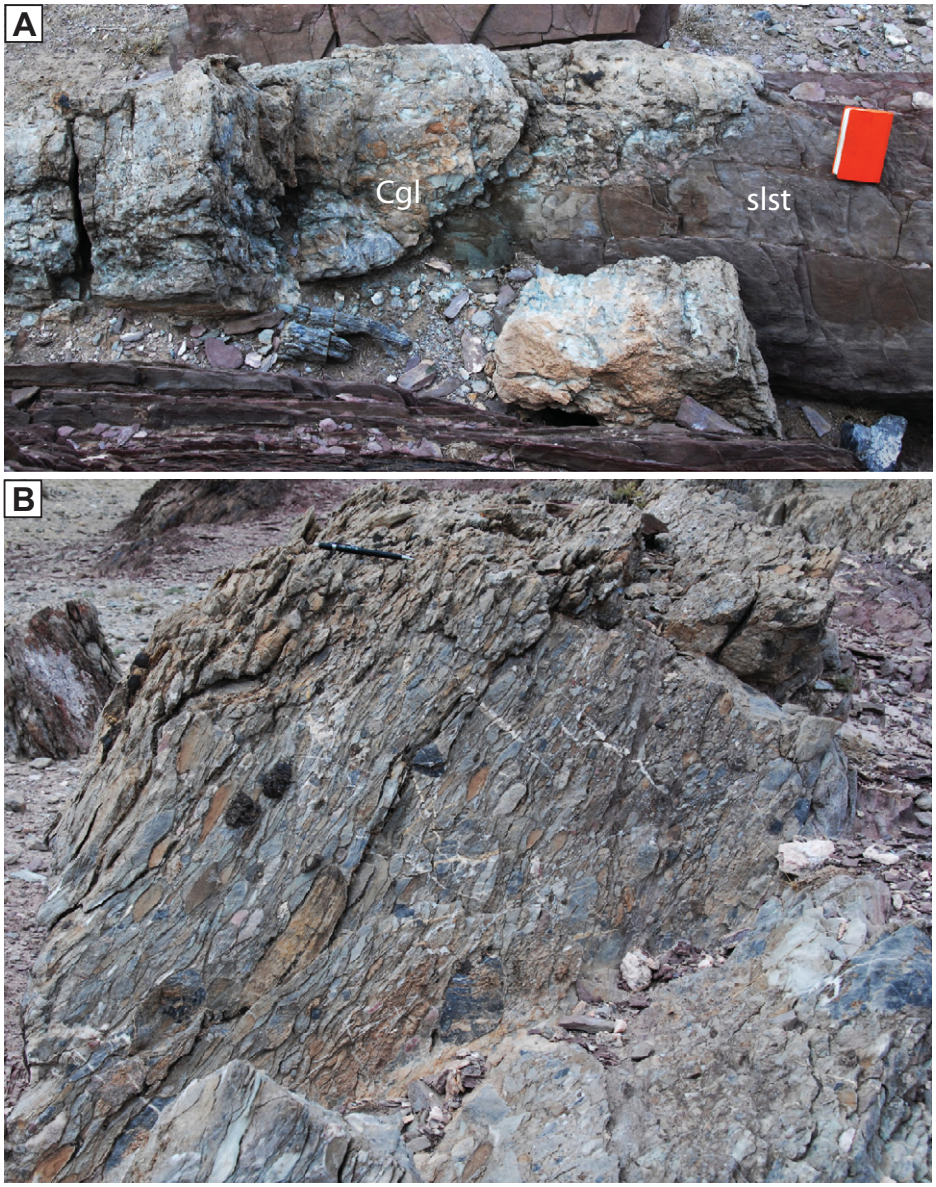

Figure 6. (A) Channel-fill deposit of pebble conglomerate within calcareous, bioturbated siltstone bed at 628 m. Note erosional contact between the conglomerate (Cgl) bed and siltstone (slst) to the left of the notebook. Notebook is 19 cm long. (B) Stretched clasts oriented roughly along bedding planes nearly parallel to cleavage in conglomerate at 610 m. Note 14-cm-long pencil near top of photo.

of the formation is interpreted as a response to tectonic subsidence, although some component of eustatic transgression cannot be ruled out. In fact, the base of the Pragian Stage is marked by a major eustatic rise, following a late Lochkovian lowstand (Johnson et al., 1985). In either case, the creation of accommodation space appears to have outpaced the rate of progradation of the fan delta. The succession of thick units of cobble conglomerate (4.2 m to 9.6 m) and rhyolitic tuff from 400 m to 502 m represents a dramatic stratigraphic shift. It is possible that seismicity and faulting were associated with local volcanism, and that these may have triggered major subaerial flows that led to deposition of these thick conglomerate units.

The stratigraphic transition into finer-grained strata directly above this conglomerate and tuff interval includes a shift to abundant red, bioturbated siltstone, which suggests that these previous events may have transformed the configuration of the basin. Changes may have included variation in the primary transport direction off the adjacent fans, which could have led to a decrease in coarse sediment influx. Alternatively, tectonic subsidence and subsequent quiescence, possibly in combination with Pragian eustatic rise, may have led to an increase of relative sea level. In addition, changes in the degree of overturn in the water body may account for the increased oxidization and bioturbation of the fine-grained facies.

Storm-Influenced Event Beds

Grading in these beds suggests that the depositing flows decelerated during deposition, and the presence of hummocky cross-stratification requires complex oscillatory flow, or combined flows with strong oscillatory flow components (velocities close to, but below, upper plane bed conditions, ~1 m/s; Southard et al., 1990; Arnott and Southard, 1990; Myrow and Southard, 1991; Dumas et al., 2005). Large, wave-generated hummocky bed forms with spacings (λ) of >1 m scale directly with wave orbital diameter (d_0), with $\lambda = 0.52d_0 + 38.5$ (Dumas et al., 2005; Yang et al., 2006). For a wavelength of hummocky cross-stratification of ~2 m, and a maximum orbital velocity for large-scale hummocky cross-stratification close to but not above ~1 m/s (Dumas et al., 2005), a calculated wave period (Komar, 1998) of ~10 s is likely for shallow to intermediate depths (Myrow et al., 2008). Ripple-scale trough cross-lamination at the tops of some beds resulted from deposition under relatively slow-moving unidirectional or combined flows. Although Airy wave theory allows for many possible combinations of water depths and wave heights, storm waves with ~10 s periods in most shallow marine basins would be associated with water depths of a few tens of meters and wave heights of a few meters to ~10 m (Myrow et al., 2008).

Interbedding of these storm-influenced beds with fine-grained background deposits reflects sporadic delivery of sediment. Transport of pebbles and sandy sediment in standing water requires steep slopes either at the shoreline of, or directly adjacent to, the depositional basin. Given the facies relationships, there was likely variable erosion and transport on the adjacent alluvial fans due to short-term weather patterns, such as seasonal runoff and storms. The coarse deposits were delivered below fair-weather wave base by powerful flows, and two likely possibilities exist for this transport.

One possibility is that coarse-grained sediment was transported into the delta front of the fan delta and was remobilized episodically as a result of slumping. In this case, retrogressive failures (Van den Berg et al., 2002) would generate mass flows in the delta front region, possibly in mouth bars. None of the event beds in this

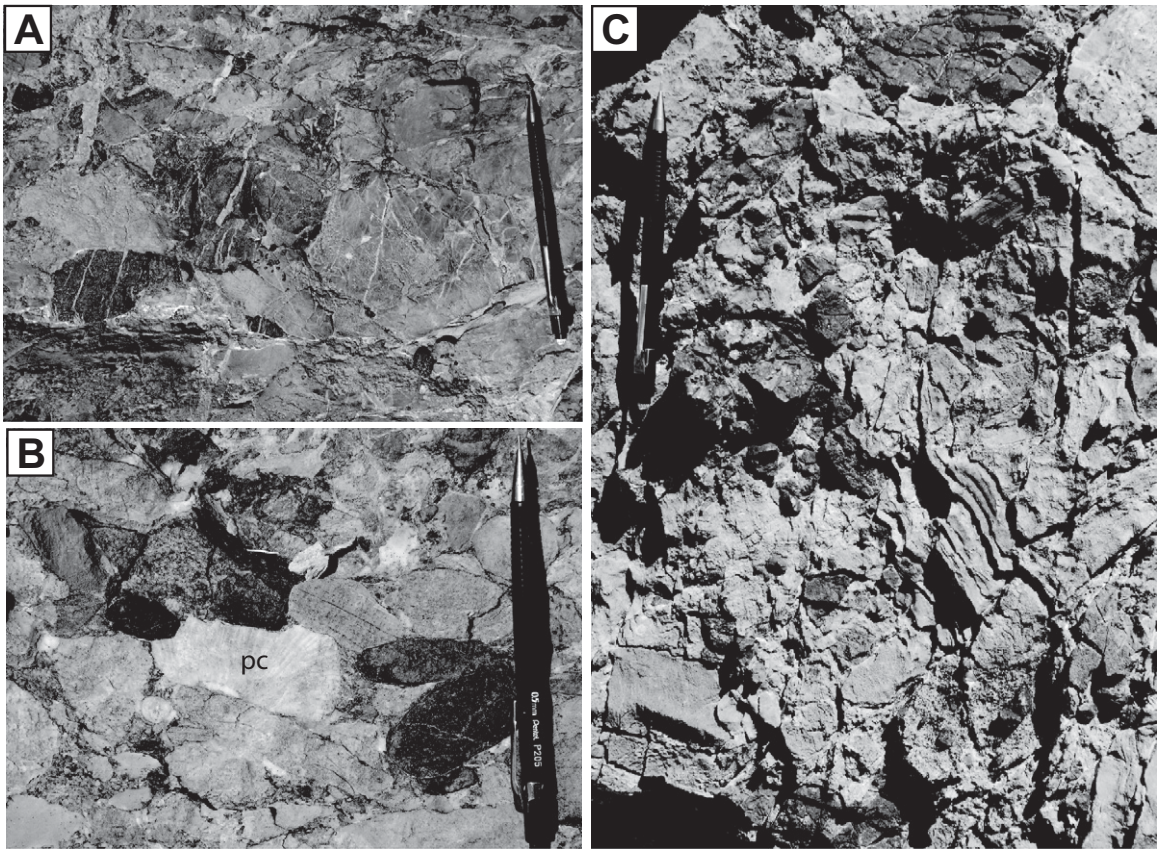

Figure 7. (A) Fractures and calcite veins within angular carbonate clasts at 501 m, some of which extend beyond the clast boundaries, whereas others appear to be contained solely within the clasts. (B) Pink coral (pc), gray carbonate, and dark dolomite clasts at 498 m. (C) Sandstone, carbonate, and dolomite clasts at 451 m. Pencil in photos is 14 cm long.

study shows evidence of deposition from high-viscosity flows (i.e., debris flows), such as massive textures and matrix-supported fabrics. In fact, the beds show clast-supported conglomeratic divisions, erosional bases, and well-defined grading and stratification. Thus, a slump origin would require flow transitions into fully turbulent currents.

A second hypothesis, consistent with the character of these beds, including their coarse grain sizes, is that they were directly related to high-energy, flood-stage input from a river mouth. In other words, these deposits would represent hyperpycnal flows that resulted from floods on the adjacent alluvial fans. In this case, the floodwaters would have exceeded the density of seawater (~35 g/L) due to excess density provided by large quantities of suspended gravel, sand, and mud (Mulder and Syvitski, 1995; Mulder et al., 2003; Lamb and Mohrig, 2009), although mixing of saline water into the hyperpycnal flow requires much less suspended sediment concentrations (Felix et al., 2006).

Fan deltas are ideal depositional systems for hyperpycnal flows since they form in fault-bounded basins in active tectonic settings with small catchment basins and short drainage systems (Mulder and Syvitski, 1995; Johnson et al., 2001; Mulder et al., 2003; Warrick and Milliman, 2003; Hicks et al., 2004). In such systems, ambient oceanographic processes such as oceanic currents, waves, and tides can modify the sediment deposited by hyperpycnal flows during and after deposition (Nittrouer and Wright, 1994). Hummocky cross-stratified hyperpycnal flow deposits would thus likely record the wave climate of the water body adjacent to the flooded landscape during the same event (M.P. Lamb et al., 2008; Myrow et al., 2008). Numerous studies have documented shallow-marine density current deposits with storm-generated stratification (i.e., "wave-modified turbidites" of Myrow et al., 2002) (e.g., Mulder et al., 2003; Plink-Björklund and Steel, 2004; Pattison, 2005; M.P. Lamb et al., 2008; Myrow et al., 2008). Gravity-driven transport of sandy or finer sediment onto shelves (Wright and Friedrichs, 2006) may be enhanced by turbulence generated at the bed by waves (Myrow and Southard, 1996), and may include fine-grained sediment suspensions that can move on relatively low slopes (Trowbridge and Kineke, 1994; Ogston and Sternberg, 1999; Kineke et al., 2000; Traykovski et al., 2000; Warrick and Milliman, 2003).

The transition within the Tsakhir Formation from the lower terrestrial cobble conglomerate deposits to shallow-marine deposits is relatively rapid, and thus there is minor stratigraphic section that might be interpreted as delta front facies. As a result, it is not readily apparent whether the coarse event beds resulted from slump-generated flows or hyperpycnal flows. The absence of slumped masses, slide scars, and debris-flow deposits favors the latter interpretation and provides another example of likely hyperpycnal flows deposited under powerful storm conditions linked to terrestrial floods.

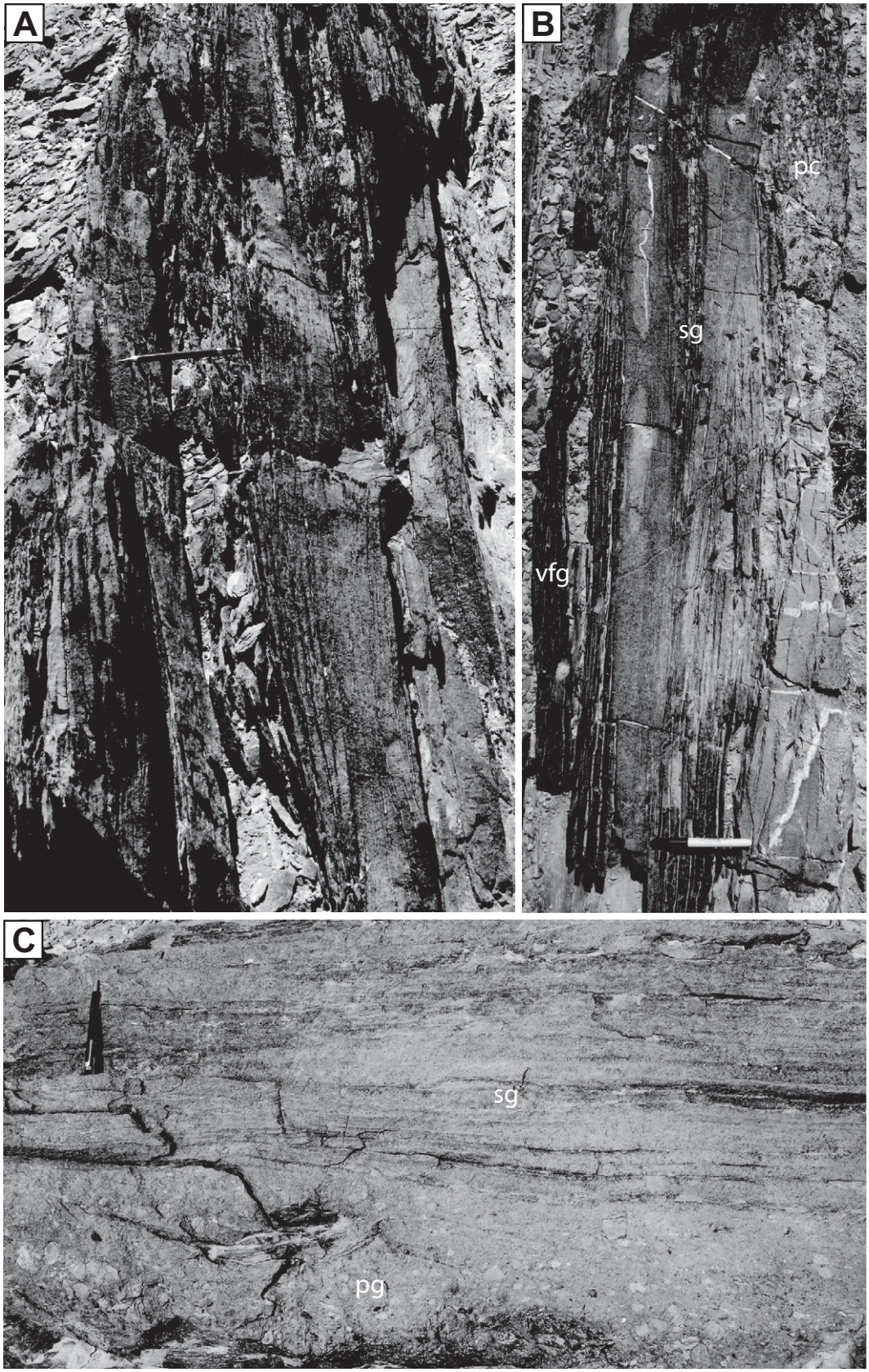

Figure 8. (A) Hummocky cross-stratified calcareous sublitharenite grading into sandy grainstone at 354 m. (B) Pebble conglomerate (pc) at base fining upward into hummocky cross-stratified sandy grainstone (sg) and then into very fine grainstone (vfg) at 322 m. (C) Pebbly grainstone (pg) fining upward into thinly bedded, sandy grainstone (sg) at 229 m. Pencil and marker in photos are 14 cm long, and their tips point up section.

Figure 9. Reduction spots and light-gray burrows on bedding surfaces in red calcareous siltstone at 604 m. Pencil tip is 2 cm long.

DETRITAL ZIRCON GEOCHRONOLOGY

Methods

Five samples were collected from the Shine Jinst region for detrital zircon geochronology. Two samples were taken from the Upper Ordovician Gashuunovoo Formation (Wang et al., 2005): SJS6–106 and SJS6–114. Sample TSA-138 was from the Lower Devonian Tsakhir Formation, and samples Ch-4d1 and Ch-4d2 were collected from the Lower Devonian Chuluun Formation (Fig. 3). Zircons from each of the five samples were separated using standard crushing and gravimetric techniques, and subpopulations for analysis were randomly selected. Zircon mounts were prepared according to standard procedures at the Arizona LaserChron laboratory (Gehrels et al., 2008).

U-Pb geochronology of detrital zircons was conducted by laser ablation–multicollector–inductively coupled plasma–mass spectrometry (LA-MC-ICP-MS) at the Arizona LaserChron Center (Appendix 1[1]). Isotopic compositions were calibrated by analyses of a Sri Lanka zircon with an age of 563.5 ± 3.2 Ma (Gehrels et al., 2008). R33 (Black et al., 2004) was analyzed with each sample and used as a secondary standard; in all cases, the average of the measured R33 ages was within 1% of the known age of ca. 419.3 Ma. Common Pb correction was based on measured ^{204}Pb, utilizing a common Pb composition from Stacey and Kramers (1975).

Errors in determining ^{206}Pb/^{238}U and ^{206}Pb/^{204}Pb for each analysis result in a measurement error of ~1%–2% (at 2Σ level) in the ^{206}Pb/^{238}U age. Errors in measurement of ^{207}Pb/^{206}Pb and ^{206}Pb/^{204}Pb also result in ~1%–2% uncertainty (at 2Σ level) in age for grains that are older than 1.0 Ga, but percentages of uncertainty are significantly larger for grains that are younger than 1.0 Ga due to low intensity of the ^{207}Pb signal.

One-hundred grains were analyzed per sample. All analyses are reported in Table DR1 (see footnote 1), except for those with high (>500 counts per second [cps]) concentrations of ^{204}Pb. Pb/U concordia plots and relative age probability plots are included in Table DR1 (see footnote 1). In the probability plots and in the following discussion, ^{206}Pb/^{238}U ages are used for analyses that are younger than 1.0 Ga, whereas ^{206}Pb/^{207}Pb ages are used for older than 1.0 Ga analyses. Data were filtered as follows: (1) ^{206}Pb/^{238}U ages younger than 1.0 Ga at 1Σ were rejected if uncertainty was >10%, (2) ^{206}Pb/^{207}Pb ages older than 1.0 Ga were rejected if uncertainty was >10%, (3) analyses older than 600 Ma were rejected if discordance was >10%, and (4) analyses older than 600 Ma were rejected if reverse discordance was >5%.

Following this filtering process, 421 analyses were retained from the original 500 analyses. A complexity with the U-Pb data set is that several analyses yielded ^{206}Pb/^{238}U ages that are younger than the minimum depositional ages for the Lower Devonian samples, which, based on the biostratigraphy of Wang et al. (2005), are 407 ± 2.8 Ma (Ogg et al., 2008) for sample TSA-138 and 391.8 ± 0.4 Ma for samples Ch-4d1 and Ch-4d2. Most of the too-young analyses have large uncertainty, suggesting that they were

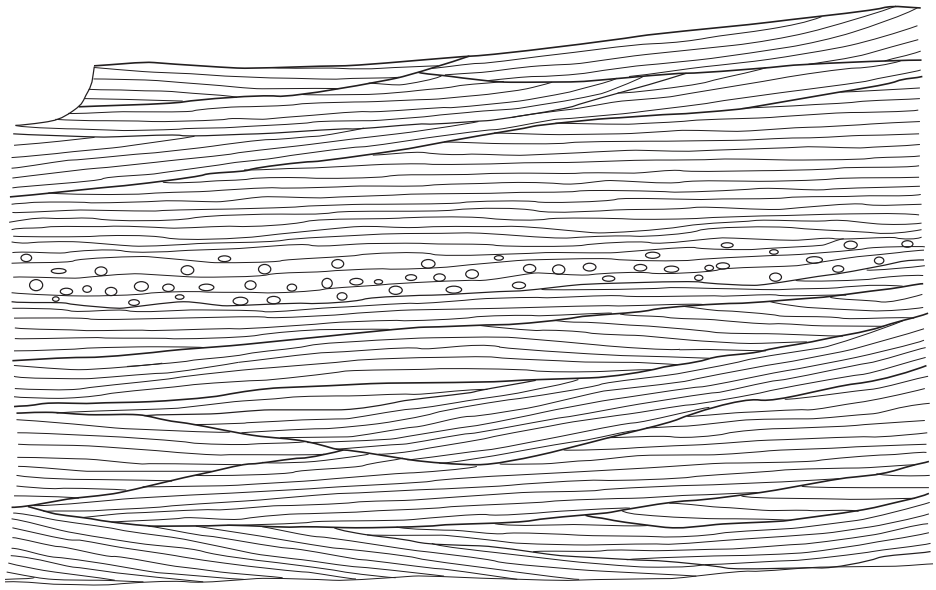

Figure 10. Sketch of hummocky cross-stratified calcareous sublitharenite beds at 354 m. Lower half consists of a sublitharenite bed, which is overlain by a graded bed with a pebbly sandstone base and hummocky cross-stratified sandstone division above.

[1]GSA Data Repository item 2013145, detrital zircon geochronologic data, is available at http://www.geosociety.org/pubs/ft2013.htm or by request to editing@geosociety.org.

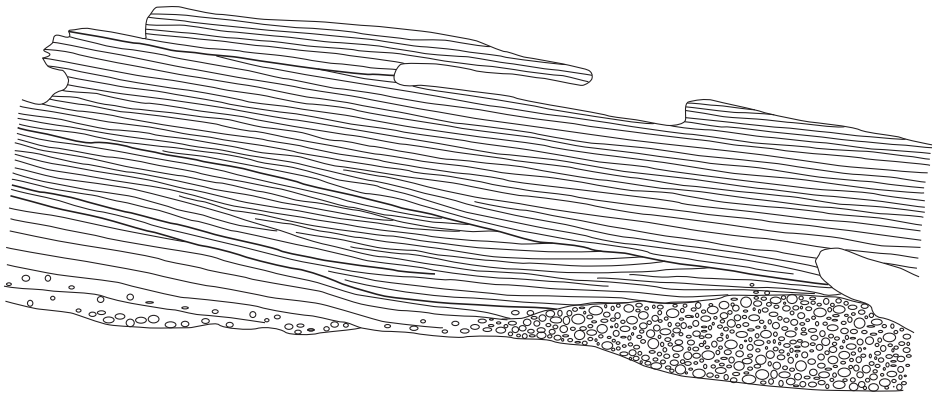

Figure 11. Sketch of complex graded bed at 352 m with a conglomeratic base, overlying hummocky cross-stratified calcareous sandstone, and upper parallel-laminated very fine sandy grainstone. Note erosional base and lateral transition from conglomerate to pebbly sandstone.

compromised by either Pb loss or intersection of fractures/inclusions during laser ablation. Only two of 421 analyses are younger than the depositional age outside of 2Σ analytical uncertainty. Such complications do not appear to have affected most analyses, given that the youngest peaks in age probability are consistent with the biostratigraphic information for all three Lower Devonian samples.

Results

The two Upper Ordovician (Ashgillian, ca. 445 Ma) Gashuunovoo samples produced zircons with a wide range of color and morphology. Most are colorless to light tan, and a few have light to medium shades of pink. The majority of grains are stubby with ~2:1 length to width ratios, and lengths average 100 µm and range up to 200 µm. The grains are mainly euhedral or anhedral/broken, although a few grains are slightly to moderately rounded. The samples are dominated by Early to Middle Cambrian (ca. 513 Ma and ca. 507 Ma) grains, although there are also Archean (ca. 3300–3160 Ma), Paleoproterozoic (ca. 2040–2010 Ma), latest Paleoproterozoic to early Mesoproterozoic (1700–1460 Ma), and Neoproterozoic (ca. 950–930 Ma and ca. 780–770 Ma) grains (Fig. 12).

The Lower Devonian Tsakhir Formation sample TSA-138 contains mostly moderately elongate grains with length to width ratios of 2:1–4:1. An approximately equal proportion of grains are either euhedral or anhedral/broken. The grains are gray, moderately rounded, and ~100 µm long. Roughly 5% of the grains are light pink, moderately rounded, and slightly smaller. The sample spectrum contains small Paleoproterozoic to Archean (ca. 2915–1900 Ma) age populations, a moderate Neoproterozoic (ca. 950–700 Ma) population, many Cambrian (ca. 500 Ma) grains, and a small proportion of Early Devonian grains (ca. 410 Ma) (Fig. 12).

Lower Devonian Chuluun Formation sample Ch-4d1 grains are colorless to light tan and dominantly euhedral (~20 are anhedral/broken). The grains are elongate, with length:width ratios of 3:1–5:1. None of the grains show any rounding, and all grains are <12 µm long. Grains in sample Ch-4d2 average 80 µm in length, although some are up to 150 µm long. Approximately half of the grains are euhedral, and the other half of the grains are broken/anhedral. None of the grains are rounded, and all grains are <120 µm long. The age spectrum for this sample includes small clusters of Archean (ca. 2920 and 2710 Ma), Mesoproterozoic (ca. 2000 Ma), and Neoproterozoic (950–750 Ma) grains. Both Chuluun samples contain significant Cambrian (ca. 522 Ma and ca. 517 Ma) and Early Devonian (ca. 411 Ma and ca. 409 Ma) populations (Fig. 12).

INTERPRETATIONS

The various aspects of the Tsakhir Formation described herein, including (1) a sharp unconformable facies contact between carbonate to coarse, alluvial-fan deposits; (2) evidence for increased subsidence; (3) volcanics; and (4) changes in basin configuration, provide a record of the onset of active tectonics within the Gobi-Altai zone during the Early Devonian. We herein name this tectonic episode the "Tsakhir event." The event corresponds with the unconformity documented by Markova (1975), which extends throughout the Gobi-Altai zone (Kröner et al., 2010). Kröner et al. (2010, their Fig. 12) depicted south-directed subduction north of the Gobi-Altai zone, north-directed subduction south of the South Gobi zone, and a back-arc region between the two blocks with down-to-the-south normal faults along the northern edge, which roughly correspond to the location of our field area (near transition from Gobi-Altai zone to Mandalovoo subzone). For this interpretation, Kröner et al. (2010) cited the work of Demoux et al. (2009b) and the identification of Early Devonian arc volcanics in the Tseel terrane, which is situated to the west of Shine Jinst along the Trans-Altai fault. However, the Tseel terrane has a structural dip to the north, with metamorphic grade increasing to the south (Demoux et al., 2009b). We find no evidence of Silurian-age south-dipping subduction under the Gobi Altai zone. We suggest either the Tsakhir event reflects (1) foreland deposition as the Gobi Altai zone collided with arc terranes to the north, or (2) the initiation of north-dipping subduction under the Gobi Altai zone and back-arc extension, in which normal faulting in the back arc may have resulted from slab roll-back, a tectonic condition commonly associated with coastal alluvial fans adjacent to marine platforms (Rust and Koster, 1984; Follo, 1992).

Although considerable longshore transport, and thus distal detrital source areas, is possible for the volumetrically minor sandstone deposits of the Upper Ordovician Gashuunovoo Formation, the Tsakhir fan-delta deposits described herein require short transport distances, and thus locally derived sediment sources. Most clasts in the Tsakhir Formation consist of lithologies represented by directly underlying carbonate deposits, but spectra from sandstone samples from the Tsakhir and both older Ordovician and younger Devonian rocks contain a wide range of zircon ages that would be typical of derivation from continental crust and/or older sedimentary rocks. The presence of quartz grains in the matrix of Tsakhir Formation conglomerate beds would support considerable local relief on newly developed faults that would have exposed quartz-rich basement rocks, presumably on the footwall of a normal fault, with possible contribution of sediment from unpreserved pre-Ordovician siliciclastic strata that were eroded at this time. In any case, the spectra for both our Upper Ordovician and Lower Devonian strata are largely similar, and thus major differences in source terrane are unlikely.

As outlined earlier, the Gobi-Altai zone is centrally located within the Central Asian orogenic belt, which formed through multiple Neoproterozoic to early Mesozoic accretionary events (Briggs et al., 2007; Windley et al., 2007; Kröner et al., 2010). Basement rocks of the Gobi-Altai zone are not exposed in the Shine Jinst region, and thus the spatial distribution of various potential basement sources is not well constrained.

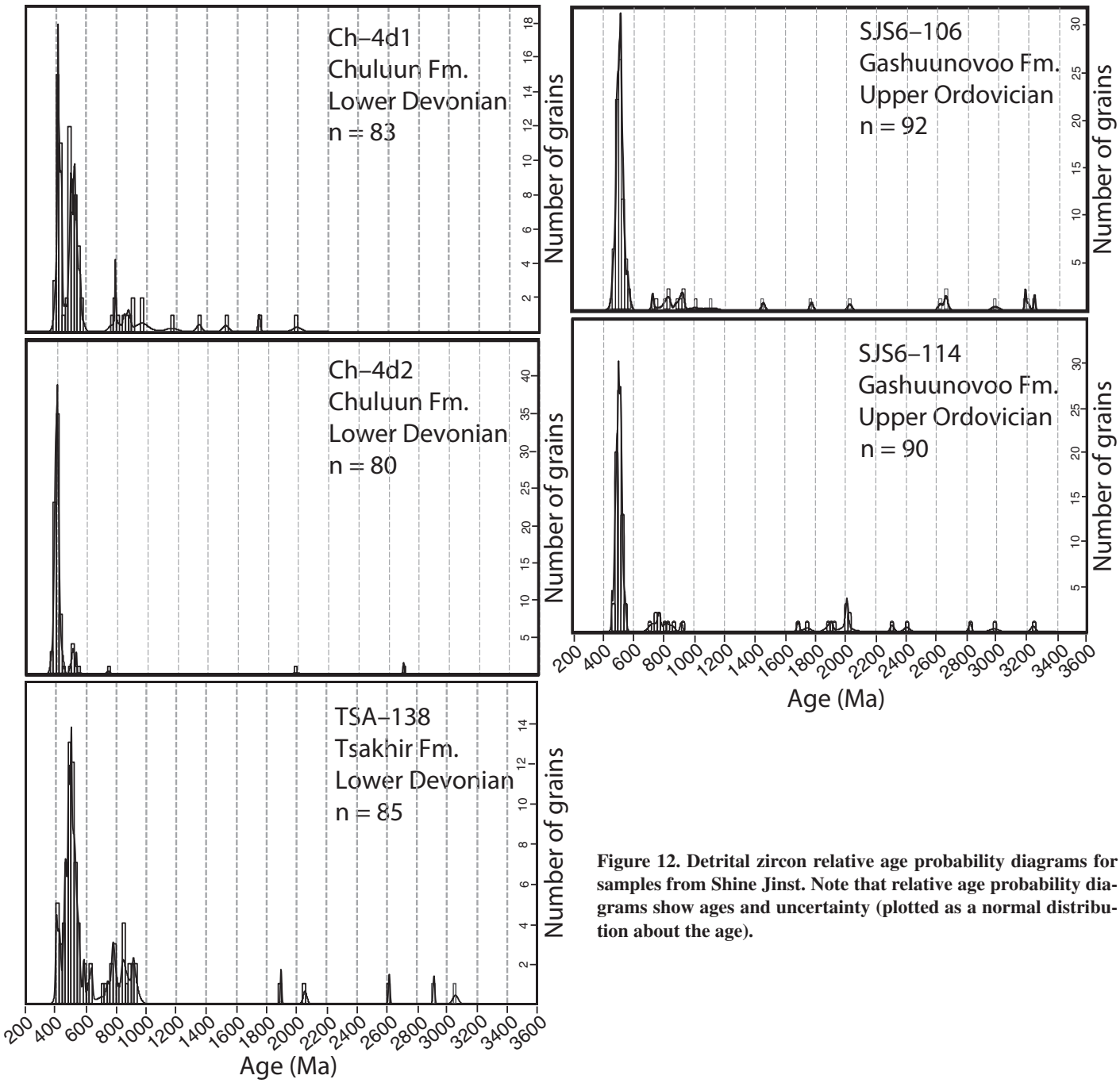

Figure 12. Detrital zircon relative age probability diagrams for samples from Shine Jinst. Note that relative age probability diagrams show ages and uncertainty (plotted as a normal distribution about the age).

The detrital zircons analyzed in this study are dominantly euhedral, and the other grains show only a slight to moderate level of rounding. The gray color and lack of abundant inclusions, and dominantly euhedral geometries, suggest that these are first-cycle grains that experienced relatively short transport. Minor differences between the spectra of Ordovician and Devonian samples may reflect changes in exposed source regions and transport paths prior to, and after, the Lower Devonian tectonic event documented in this study. For instance, the Devonian samples have little (Ch-4d1) or no (Ch-4d2, TSA-138) ca. 1000–1800 Ma grains, whereas grains of these ages are moderately abundant in Ordovician samples. In addition, although all samples are dominated by young zircons, the gap between the youngest grains and the depositional ages of the Devonian samples is smaller (<~5 m.y.) than for Ordovician samples (<~30 m.y.). The small age gap for Devonian samples reflects relatively rapid incorporation of eroded felsic igneous grains that were derived relatively locally from volcanic centers within this active tectonic setting. The small gap is consistent with deposition within an active convergent margin where uplift and erosion took place shortly after deposition (Cawood et al., 2012).

Local basement of the Gobi-Altai zone may have tectonic affinities with nearby basement north of the Main Mongolian lineament. The most prominent peaks in the Ordovician and Early Devonian samples from the Gobi-Altai

zone are middle Neoproterozoic (ca. 800 Ma) and Cambrian, with a prominent gap between them. This spectral pattern corresponds with widespread ca. 800 Ma continental arc volcanism on the Mongolian microcontinent (Kuzmichev et al., 2001, 2005; Kelty et al., 2008; Levashova et al., 2010), rifted passive margin development between 750 and 580 Ma, and syn- to postorogenic granite formation during the Cambrian Salarian orogeny (Ruzhentsev and Burashnikov, 1996; Buchan et al., 2002; Khain et al., 2003; Demoux et al., 2009a; Macdonald et al., 2009). Although late Neoproterozoic zircon ages have been reported from Mongolia (e.g., Buchan et al., 2002; Khain et al., 2003; Demoux et al., 2009a), these are from plagiogranite veins in ophiolites and are volumetrically insignificant for detrital zircon production compared to the vast area of the Mongolian microcontinent, which is mantled by ca. 800 Ma intermediate volcanic rocks and intruded by ca. 540–500 Ma granites. In summary, our data contain peaks that coincide with basement ages and magmatic events on the adjacent Mongolian microcontinent and thus suggest that crust of similar character is present in the Gobi-Altai zone, and acted as a sediment source for our strata.

Mongolian continental fragments, including the basement of the Gobi-Altai zone, may have originated as part of eastern Gondwana or any of the cratonic domains bordering the Central Asian orogenic belt, namely, Baltica, Siberia, Tarim, and North China. Comparisons of our spectra with these cratonic domains may provide constraints for potential sources of basement rocks of the Gobi-Altai zone. Rojas-Agramonte et al. (2011) provided a compilation of detrital and xenocrystic zircon ages from Neoproterozoic to Paleozoic terranes of Mongolia, and concluded that these have tectonic affinities with Tarim and possibly Gondwanaland. They rejected Siberia and North China as possible sources because these regions lack evidence for major crust-forming events after ca. 1600 Ma. However, if Mongolian continental fragments rifted away from a parent body in the Neoproterozoic as previously suggested (Kuzmichev et al., 2001, 2005; Macdonald et al., 2009), spectral peaks younger than Neoproterozoic would not be useful for provenance links to these continents.

With regard to the Siberian craton, it contains ca. 3400 Ma metamorphosed crust, ca. 2700–2500 Ma granulites, orthogneisses, and granitoids, and localized ca. 2400, 1880, and 1850 Ma granite bodies (Sal'nikova et al., 1997; Poller et al., 2005). Southeastern Siberian basement contains ca. 2100–1850 Ma and >2300 Ma provinces (Frost et al., 1998; Khudoley and Prokopiev, 2007). Our detrital spectra from Mongolia contain small Archean and Paleoproterozoic peaks, some of which are similar to those described above for Siberia.

The compilation of grain ages for Siberia presented in Rojas-Agramonte et al. (2011) shows no grains younger than ca. 1700 Ma. However, spectra from terminal Neoproterozoic strata of the Sette Daban region of Siberia presented by MacLean et al. (2009) have multiple age populations between ca. 1700 Ma and 1000 Ma, and minor Neoproterozoic grains. Thus, even though Siberia shows little or no evidence for major crust-forming events younger than 1600 Ma, younger sedimentary grains accumulated on the craton in the Mesoproterozoic and Neoproterozoic. If parts of Mongolia were in depositional continuity with Siberia, and equivalent sedimentary successions were deposited in Mongolia, then these could have been a source of recycled detrital zircons of this age in our Ordovician Mongolian spectra, which include some ca. 1700–1200 Ma grains. Spectra for our Devonian Mongolian samples contain a gap in ages between ca. 1700 Ma and 900 Ma, and our Ordovician spectra show a gap between ca. 1200 Ma and 1000 Ma, which is anomalous if Siberia was a sediment source area.

Rojas-Agramonte et al. (2011) presented a similar argument for rejecting North China as a possible source region for Mongolian terranes, namely, the absence of crust-forming events after ca. 1600 Ma. However, McKenzie et al. (2011) presented detrital zircon spectra for Cambrian samples from both the southern and eastern margin of North China that contain a full suite of grain ages from ca. 2000 Ma to 500 Ma. In northwest China, numerous studies have described various ca. 500–400 Ma igneous bodies (W.J. Xiao et al., 2009a; Chen et al., 2010; Li et al., 2010; Long et al., 2010; Wong et al., 2010; W. Xiao et al., 2010). The presence of large populations of grains younger than ca. 1600 Ma undermines the argument that Mongolian terranes could not have been genetically linked to the North China craton. North China spectra from McKenzie et al. (2011) also include abundant ca. 1050–900 Ma grains that were either derived from unknown Grenville sources in North China or were carried from adjacent regions (i.e., Gondwanaland) by fluvial transport. Furthermore, they demonstrate no statistically significant difference in source material between Bhutanese (Gondwanan) and North China spectra. Because all of our Mongolian samples yield similar Proterozoic to lower Paleozoic (ca. 2000–500 Ma) grains to those found in North China, and since North China and Gondwanan detrital source signatures are indistinguishable from one another, parts of Mongolia could have Gondwanan affinities, in part or wholly through its connection with North China.

Myrow et al. (2010) suggested that great distances of sediment transport and high degrees of mixing of detrital zircon ages took place across the Gondwanan supercontinent, resulting in relatively homogeneous detrital zircon spectra. Detrital zircon spectra from Lower Cambrian to Middle Ordovician strata across the Himalaya from Pakistan to Bhutan include common ca. 3150, ca. 2500, and 1500–1400 Ma grain populations and many ca. 1150, 1000, 950, and 800 Ma grain populations. The uniformity of detrital signals in Gondwanaland is thought to have arisen from a combination of widespread mountain building during assembly of the supercontinent, and the development of extraordinarily large sediment dispersal systems across a nonvegetated landscape (Squire et al., 2006; Myrow et al., 2010). With regard to a possible tectonic affinity of the Gobi-Altai zone, the spectra from this study are similar to those from sedimentary successions of the northern margin of Gondwanaland, and thus they suggest a possible connection between these regions. Therefore, although the northern margin of Gondwanaland and the North China craton lack ca. 1050–900 Ma basement, grains of this age that originated from distant sources in Gondwanaland could have been deposited in Mongolia (and North China) and later been recycled and redeposited during the early to middle Paleozoic. Such a model would run counter to that of Rojas-Agramonte et al. (2011) and others who suggested that Mongolian terranes would have separated from Gondwana by the time of Grenville tectonism. We suggest, however, that it is possible that ca. 1050–900 Ma grains in Mongolian terranes could have had the same sources as those that provide a uniform and widespread signal of the same age in the Himalaya (Myrow et al., 2010), and thus separated from Gondwana after this time.

Baltica represents another possible source area for Mongolian crust. Scattered Archean and Paleoproterozoic grain ages, including peaks at ca. 2970–2600 and ca. 2120–1880 Ma, are present in detrital samples from the Svecofennian Domain of Baltica (Claesson et al., 1993; Cawood et al., 2007). Precambrian detrital zircon samples from Baltica show a ca. 700–600 Ma peak, and a wide spectrum of 2000–1000 Ma grains with large peaks from ca. 1900 Ma to 1400 Ma (Bingen et al., 2005; Cawood et al., 2007). Our Mongolian Ordovician spectra also contain small peaks or gaps in grains of this age, and for this reason, Baltica is a less likely source for crust of the Gobi-Altai zone.

The Tarim craton also represents a likely source area for Mongolian crust and associated

detrital zircon spectra (Rojas-Agramonte et al., 2011). Much of the Tarim craton consists of igneous and metamorphic rocks with ca. 2800–2500, ca. 2450–2350, and ca. 2100–1700 Ma ages, as well as ca. 1050–900 Ma ages (Hu et al., 2000; Lu et al., 2008). Proterozoic strata in Tarim yield mainly ca. 2000–1900, ca. 1900–1100, and ca. 930–820 Ma detrital zircon ages (Gehrels et al., 2003). Detrital spectra from our Ordovician and Devonian samples are consistent with both potential source rocks and detrital ages from Tarim, so it is also possible that Gobi-Altai basement originated as part of the Tarim craton.

In summary, Siberia, North China, eastern Gondwana, Baltica, and Tarim all contain potential source rocks with ages similar to our Gobi-Altai detrital spectra, including 1050–900 Ma grains. It is possible that the Gobi-Altai could be a sliver of crust that originated as part of any of these cratons, although detrital age spectra and bedrock ages in Baltica and Siberia make them less likely source regions for Gobi-Altai crust. The similarity of detrital spectra derived from samples from Gondwanaland and peri-Gondwanan crustal blocks for late Neoproterozoic through middle Paleozoic strata (e.g., Myrow et al., 2010) raises doubt about the utility of detrital spectra for discerning the affinities of terranes at this particular time in Earth history.

CONCLUSIONS

We document a complex record of early to middle Paleozoic marine carbonate deposition, tectonic uplift, and volcanism within the poorly understood Gobi-Altai zone of the Central Asian orogenic belt. This study provides the first detailed sedimentological analysis of Lower Devonian strata of the Gobi-Altai zone. A sharp unconformable contact at the base of the Lower Devonian Tsakhir Formation in the Shine Jinst region of southern Mongolia records an important tectonic change from quiescent, shallow-marine carbonate deposition during the Ordovician through earliest Devonian into syntectonic subaerial to marine coastal alluvial fan-delta complex deposition. This Tsakhir event is an important regional tectonic shift that records alluvial-fan deposition, basin subsidence, and volcanism.

A 90-m-thick basal cobble conglomerate with quartz-rich sandstone matrix represents proximal alluvial-fan deposits. The conglomerate formed in response to uplift associated with range-bounding faults that led to unroofing of underlying carbonate strata and erosion of basement rocks. These coarse fan deposits grade into fan-delta deposits with event beds, which were deposited in a shallow-marine depositional system. Some such beds contain lower divisions with pebble conglomerate that grades into fine grainstone and/or sandstone that exhibits hummocky cross-stratification, and these are capped by fine-grained suspension deposits. They also show evidence for both transport of coarse sediment by gravity flows and reworking of sandy sediment by storm-generated waves. Sedimentological analysis suggests that these beds may represent hyperpycnal flows deposited within a storm-influenced shelf, and that floods developed on alluvial fans were dynamically linked to storm events in the adjacent seaway.

Stratigraphic changes reflect the evolution of the fan-delta system and basin, including the introduction of felsic volcanic flows and ash beds. A general upward-fining pattern is punctuated by the sudden appearance of coarse conglomerate and volcanic units at ~400 m, followed at ~500 m by a transition to predominantly finer-grained, burrowed, and oxidized sediment. These stratigraphic patterns may reflect a tectonically induced change in overall basin configuration that led to both deepening and increased circulation of the water column.

We present the first detailed detrital zircon geochronologic analysis for the Gobi-Altai zone. Our analyses are from a suite of five samples covering Upper Ordovician through Lower Devonian strata. Spectra from these strata are dominated by Paleozoic grains, but they also contain a small to moderate peak of ca. 1000–700 Ma grains, and scattered Archean to Neoproterozoic grains. Both Ordovician and Devonian samples contain grains very close to their age of deposition, particularly the Devonian strata. This indicates rapid incorporation of grains derived from relatively contemporaneous igneous activity, such as subduction-related volcanism within an active convergent margin that underwent rapid uplift and erosion (Cawood et al., 2012). Other differences, including the presence of ca. 1800–1000 Ma grains in Ordovician samples, and a general absence of grains of this age in our Devonian samples, suggest changes in source regions and/or transport paths prior to, and after, the Tsakhir event.

Sedimentological and stratigraphic data of the Lower Devonian Tsakhir Formation suggest derivation of sediment from local basement and cover rocks. Similarities between our detrital age spectra and both recently published spectra and basement rock ages of the adjacent landmasses, namely, Siberia, Baltica, North China, eastern Gondwana, and Tarim, suggest that the Gobi-Altai terrane may have tectonic affinities to any of these cratons. These similarities, and those documented for late Neoproterozoic to middle Paleozoic rocks across Gondwanaland and adjacent terranes, raise questions about the use of detrital spectra for determining the tectonic affinities of crustal blocks at this time in Earth history.

ACKNOWLEDGMENTS

We acknowledge the support of the KECK Foundation and the National Science Foundation. We thank the LaserChron Laboratory staff for help with collection and analysis of the detrital zircon data. We thank Sam Bowring for use of the Massachusetts Institute of Technology laboratory, and for technical assistance and advice. We would also like to thank Constance Soja and Jeffrey Over for their assistance in coordinating and executing the field work for this study. The authors appreciate the efforts of four anonymous reviewers and editors Christian Koeberl, Fernando Corfu, and Peter Cawood.

REFERENCES CITED

Arnott, R.W., and Southard, J.B., 1990, Exploratory flow-duct experiments on combined-flow bed configurations, and some implications for interpreting storm-event stratification: Journal of Sedimentary Research, v. 60, p. 211–219.

Badarch, G., Cunningham, W.D., and Windley, B.F., 2002, A new terrane subdivision for Mongolia: Implications for the Phanerozoic crustal growth of Central Asia: Journal of Asian Earth Sciences, v. 21, p. 87–110, doi:10.1016/S1367-9120(02)00017-2.

Bingen, B., Griffin, W.L., Torsvik, T.H., and Saeed, A., 2005, Timing of late Neoproterozoic glaciation on Baltica constrained by detrital zircon geochronology in the Hedmark Group, south-east Norway: Terra Nova, v. 17, p. 250–258, doi:10.1111/j.1365-3121.2005.00609.x.

Black, L., Kamo, S., Allen, C., Davis, D., Aleinikoff, J., Valley, J., Mundil, R., Campbell, I., Korsch, R., Williams, I., and Foudoulis, C., 2004, Improved $^{206}Pb/^{238}U$ microprobe geochronology by the monitoring of a trace-element–related matrix effect; SHRIMP, ID-TIMS, ELA-ICP-MS, and oxygen isotope documentation for a series of zircon standards: Chemical Geology, v. 205, p. 115–140, doi:10.1016/j.chemgeo.2004.01.003.

Briggs, S.M., Yin, A., Manning, C.E., Chen, Z., Wang, X., and Grove, M., 2007, Late Paleozoic tectonic history of the Ertix fault in the Chinese Altai and its implications for the development of the Central Asian orogenic system: Geological Society of America Bulletin, v. 119, p. 944–960, doi:10.1130/B26044.1.

Briggs, S.M., Yin, A., Manning, C.E., Chen, Z., and Wang, X., 2009, Tectonic development of the southern Chinese Altai Range as determined by structural geology, thermobarometry, $^{40}Ar/^{39}Ar$ thermochronology, and Th/Pb ion-microbe monazite geochronology: Geological Society of America Bulletin, v. 121, p. 1381–1393, doi:10.1130/B26385.1.

Buchan, C., Pfänder, J., Kröner, A., Brewer, T.S., Tomurtogoo, O., Tomurhuu, D., and Cunningham, W.D., 2002, Timing of accretion and collision deformation in the Central Asian orogenic belt: Implications of granite geochronology in the Bayankhongor ophiolite zone: Chemical Geology, v. 192, p. 23–45, doi:10.1016/S0009-2541(02)00138-9.

Cawood, P.A., Nemchin, A.A., Strachan, R., Prave, T., and Krabbendam, M., 2007, Sedimentary basin and detrital zircon record along East Laurentia and Baltica during assembly and breakup of Rodinia: Geological Society of America Bulletin, v. 164, p. 257–275.

Cawood, P.A., Hawkesworth, C.J., and Dhuime, B., 2012, Detrital zircon record and tectonic setting: Geology, v. 40, p. 875–878, doi:10.1130/G32945.1.

Chen, J.F., Han, B.F., Ji, J.Q., Zhang, L., Xu, Z., He, G.Q., and Wang, T., 2010, Zircon U-Pb ages and tectonic implications of Paleozoic plutons in northern West Junggar, North Xinjiang, China: Lithos, v. 115, p. 137–152, doi:10.1016/j.lithos.2009.11.014.

Claesson, S., Huhma, H., Kinny, P., and Williams, I.S., 1993, Svecofennian detrital zircon ages—Implications for the

evolution of the Baltic Shield: Precambrian Research, v. 64, p. 109–130, doi:10.1016/0301-9268(93)90071-9.

Cunningham, W.D., 2010, Tectonic setting and structural evolution of the late Cenozoic Gobi Altai orogen, *in* Kusky, T.M., Zhai, M.-G., and Xiao, W., eds., The Evolving Continents: Understanding Processes of Continental Growth: Geological Society of London Special Publication 338, p. 361–387, doi:10.1144/SP338.17.

Daily, B., Moore, P.S., and Rust, B.R., 1980, Terrestrial-marine transition in the Cambrian rocks of Kangaroo Island, South Australia: Sedimentology, v. 27, p. 379–399, doi:10.1111/j.1365-3091.1980.tb01189.x.

Demoux, A., Kröner, A., Badarch, G., Jian, P., Tomurhuu, D., and Wingate, W.T.D., 2009a, Zircon ages from the Baydrag block and the Bayankhongoor ophiolite zone: Time constraints on late Neoproterozoic to Cambrian subduction- and accretion-related magmatism in central Mongolia: The Journal of Geology, v. 117, p. 377–397, doi:10.1086/598947.

Demoux, A., Kröner, A., Hegner, E., and Badarch, G., 2009b, Devonian arc magmatism in the Tseel terrane of SW Mongolia: Chronological and geochemical evidence: Journal of the Geological Society of London, v. 166, p. 459–471, doi:10.1144/0016-76492008-090.

Dumas, S., Arnott, R.W.C., and Southard, J.B., 2005, Experiments on oscillatory-flow and combined-flow bed forms: Implications for interpreting parts of the shallow-marine sedimentary record: Journal of Sedimentary Research, v. 75, p. 501–513, doi:10.2110/jsr.2005.039.

Felix, M., Peakall, J., and McCaffrey, W.D., 2006, Relative importance of processes that govern the generation of particulate hyperpycnal flows: Journal of Sedimentary Research, v. 76, p. 382–387, doi:10.2110/jsr.2006.022.

Follo, M.F., 1992, Conglomerates as clues to the sedimentary and tectonic evolution of a suspect terrane: Wallowa Mountains, Oregon: Geological Society of America Bulletin, v. 104, p. 1561–1576, doi:10.1130/0016-7606(1992)104<1561:CACTTS>2.3.CO;2.

Frost, B.R., Avchenko, O.V., Chaberlain, K.R., and Frost, C.D., 1998, Evidence for extensive Proterozoic remobilization of the Aldan shield and implications for Proterozoic plate tectonic reconstructions of Siberia and Laurentia: Precambrian Research, v. 89, p. 1–23, doi:10.1016/S0301-9268(97)00074-0.

Gehrels, G.E., Yin, A., and Wang, X.F., 2003, Detrital-zircon geochronology of the northeastern Tibetan Plateau: Geological Society of America Bulletin, v. 115, p. 881–896, doi:10.1130/0016-7606(2003)115<0881:DGOTNT>2.0.CO;2.

Gehrels, G.E., Valencia, V., and Ruiz, J., 2008, Enhanced precision, accuracy, efficiency, and spatial resolution of U-Pb ages by laser ablation–multicollector–inductively coupled plasma–mass spectrometry: Geochemistry Geophysics Geosystems, v. 9, p. Q03017, doi:10.1029/2007GC001805.

Heubeck, C., 2001, Assembly of central Asia during the middle and late Paleozoic, *in* Hendrix, M.S., and Davis, G.A., eds., Paleozoic and Mesozoic Tectonic Evolution of Central and Eastern Asia: From Continental Assembly to Intracontinental Deformation: Geological Society of America Memoir 194, p. 1–22.

Hicks, D.M., Gomez, B., and Trustrum, N.A., 2004, Event suspended sediment characteristics and the generation of hyperpycnal plumes at river mouths: East Coast continental margin, North Island, New Zealand: The Journal of Geology, v. 112, p. 471–485, doi:10.1086/421075.

Hu, A., Jahn, B-m, Zhang, G., Chen, Y., and Zhang, Q., 2000, Crustal evolution and Phanerozoic crustal growth in northern Xinjiang: Nd isotopic evidence. Part I. Isotopic characterization of basement rocks: Tectonophysics, v. 328, p. 15–51.

Jo, H.R., Rhee, C.W., and Chough, S.K., 1997, Distinctive characteristics of a streamflow-dominated alluvial fan deposit: Sanghori area, Kyongsang Basin (Early Cretaceous), southeastern Korea: Sedimentary Geology, v. 110, p. 51–79, doi:10.1016/S0037-0738(96)00083-8.

Johnson, C.L., Amory, J.A., Zinniker, D., Lamb, M.A., Graham, S.A., Affolter, M., and Badarch, G., 2008, Sedimentary response to arc-continent collision, Permian, southern Mongolia, *in* Draut, A.E., Clift, P.D., and Scholl, D.W., eds., Formation and Applications of the Sedimentary Record in Arc Collision Zones: Geological Society of America Special Paper 436, p. 363–390.

Johnson, J.G., Klapper, G., and Sandberg, C.A., 1985, Devonian eustatic fluctuations in Euramerica: Geological Society of America Bulletin, v. 96, p. 567–587, doi:10.1130/0016-7606(1985)96<567:DEFIE>2.0.CO;2.

Johnson, K.S., Paull, C.K., Barry, J.P., and Chavez, F.P., 2001, A decadal record of underflows from a coastal river into the deep sea: Geology, v. 29, p. 1019–1022, doi:10.1130/0091-7613(2001)029<1019:ADROUF>2.0.CO;2.

Kelty, T.K., Yin, A., Dash, B., Gehrels, G.E., and Ribeiro, A.E., 2008, Detrital-zircon geochronology of Paleozoic sedimentary rocks in the Hangay-Hentey basin, north-central Mongolia: Implications for the tectonic evolution of the Mongol-Okhotsk Ocean in central Asia: Tectonophysics, v. 451, p. 290–311, doi:10.1016/j.tecto.2007.11.052.

Khain, E.V., Bibikova, E.V., Salnikova, E.B., Kröner, A., Gibsher, A.S., Didenko, A.N., Degtyarev, K.E., and Fedotova, A.A., 2003, The Palaeo–Asian Ocean in the Neoproterozoic and early Palaeozoic. New geochronologic data and palaeotectonic reconstructions: Precambrian Research, v. 122, p. 329–358, doi:10.1016/S0301-9268(02)00218-8.

Khudoley, A.K., and Prokopiev, A.V., 2007, Defining the eastern boundary of the North Asian craton from structural and subsidence history studies of the Verkhoyansk fold-and-thrust belt, *in* Sears, J.W., Harms, T.A., and Evenchick, C.A., eds., Whence the Mountains? Inquiries into the Evolution of Orogenic Systems: A Volume in Honor of Raymond A. Price: Geological Society of America Special Paper 433, p. 391–410.

Kim, S.B., Chough, S.K., and Chun, S.S., 1995, Bouldery deposits in the lowermost part of the Cretaceous Kyokpori Formation, SW Korea: Cohesionless debris flows and debris falls on a steep-gradient delta slope: Sedimentary Geology, v. 98, p. 97–119, doi:10.1016/0037-0738(95)00029-8.

Kineke, G.C., Woolfe, K.J., Kuel, S.A., Milliman, J.D., Dellapenna, T.M., and Purdon, R.G., 2000, Sediment export from the Sepik River, Papua New Guinea: Evidence for a divergent sediment plume: Continental Shelf Research, v. 20, p. 2239–2266, doi:10.1016/S0278-4343(00)00069-8.

Komar, P.D., 1998, Beach Processes and Sedimentation: Upper Saddle River, New Jersey, Prentice Hall, 543 p.

Kröner, A., Lehmann, J., Schulmann, K., Demoux, A., Lexa, O., Tomurhuu, D., Stipská, P., Liu, D.Y., and Wingate, M.T.D., 2010, Lithostratigraphic and geochronological constraints on the evolution of the Central Asian orogenic belt in SW Mongolia: Early Paleozoic rifting followed by late Paleozoic accretion: American Journal of Science, v. 310, p. 523–574, doi:10.2475/07.2010.01.

Kuzmichev, A., Bibikova, E.V., and Zhuravlev, D.Z., 2001, Neoproterozoic (~800 Ma) orogeny in the Tuva-Mongolia Massif (Siberia): Island arc–continent collision at the northeast Rodinia margin: Precambrian Research, v. 110, p. 109–126, doi:10.1016/S0301-9268(01)00183-8.

Kuzmichev, A., Kröner, A., Liu, D.Y., and Wan, Y.S., 2005, The Shishkhid ophiolite, northern Mongolia: A key to the reconstruction of a late Neoproterozoic island-arc system in central Asia: Precambrian Research, v. 138, p. 125–150, doi:10.1016/j.precamres.2005.04.002.

Lamb, M.A., and Badarch, G., 1997, Paleozoic sedimentary basins and volcanic-arc systems of southern Mongolia: New stratigraphic and sedimentologic constraints: International Geology Review, v. 39, p. 542–576, doi:10.1080/00206819709465288.

Lamb, M.A., and Badarch, G., 2001, Paleozoic sedimentary basins and volcanic arc systems of southern Mongolia: New geochemical and petrographic constraints, *in* Hendrix, M.S., and Davis, G., eds., Paleozoic and Mesozoic Tectonic Evolution of Central Asia: From Continental Assembly to Intracontinental Deformation: Geological Society of America Memoir 194, p. 117–149.

Lamb, M.A., Badarch, G., Navratil, T., and Poier, R., 2008, Structural and geochronologic data from the Shine Jinst area, eastern Gobi Altai, Mongolia: Implications for Phanerozoic intracontinental deformation in Asia: Tectonophysics, v. 451, p. 312–330, doi:10.1016/j.tecto.2007.11.061.

Lamb, M.P., and Mohrig, D., 2009, Do hyperpycnal-flow deposits record river-flood dynamics?: Geology, v. 37, p. 1067–1070, doi:10.1130/G30286A.1.

Lamb, M.P., Myrow, P.M., Lukens, C., Houck, K., and Strauss, J., 2008, Deposits from wave-influenced turbidity currents: Pennsylvanian Minturn Formation, Colorado, USA: Journal of Sedimentary Research, v. 78, p. 480–498, doi:10.2110/jsr.2008.052.

Levashova, N.M., Kalugin, V.M., Gibsher, A.S., Ryabinin, J., Yff, A.B., Meert, J.G., and Malone, S.J., 2010, The origin of the Baydaric microcontinent, Mongolia: Constraints from paleomagnetism and geochronology: Tectonophysics, v. 485, p. 306–320.

Li, Z., Li, Y., Chen, H., Santosh, M., Xiao, W., and Wang, H., 2010, SHRIMP U-Pb zircon chronology of ultra-high-temperature spinel-orthopyroxene-garnet granulite from South Altay orogenic belt, northwestern China: The Island Arc, v. 19, p. 506–516, doi:10.1111/j.1440-1738.2010.00726.x.

Long, X., Yuan, C., Sun, M., Xiao, W., Zhao, G., Wang, Y., Cai, K., Xia, X., and Xie, L., 2010, Detrital zircon ages and Hf isotopes of the early Paleozoic flysch sequence in the Chinese Altai, NW China: New constrains on depositional age, provenance and tectonic evolution: Tectonophysics, v. 480, p. 213–231, doi:10.1016/j.tecto.2009.10.013.

Lu, S., Li, H., Zhang, C., and Nlu, G., 2008, Geological and geochronological evidence for the Precambrian evolution of the Tarim craton and surrounding continental fragments: Precambrian Research, v. 160, p. 94–107, doi:10.1016/j.precamres.2007.04.025.

Macdonald, F.A., Jones, D.S., and Schrag, D.P., 2009, Stratigraphic and tectonic implications of a new glacial diamictite-cap carbonate couplet in southwestern Mongolia: Geology, v. 37, p. 123–126, doi:10.1130/G24797A.1.

MacLean, J.S., Sears, J.W., Chamberlain, K.R., Khudoley, A.K., Prokopiev, A.V., Kropachev, A.P., and Serkina, G.G., 2009, Detrital zircon geochronologic test of the SE Siberia–SW Laurentia paleocontinent connection, *in* Stone, D.B., Fujita, K., Layer, P.W., Miller, E.L., Prokopiev, A.V., and Toro, J., eds., Geology, Geophysics and Tectonics of Northeastern Russia: A Tribute to Leonid Parfenov: Stephan Mueller Special Publication Series, v. 4, p. 111–116.

Major, J.J., 1997, Depositional processes in large-scale debris-flow experiments: The Journal of Geology, v. 105, p. 345–366, doi:10.1086/515930.

Markova, N.G., 1975, Stratigraphy of the Lower and Middle Paleozoic of Western Mongolia: Moscow, Nauka Press, Transactions of Joint Soviet-Mongolian Scientific Research Geological Expedition, v. 12, p. 119.

McKenzie, N.R., Hughes, N.C., Myrow, P.M., Choi, D.K., and Park, T., 2011, Trilobites and zircons link north China with the eastern Himalaya during the Cambrian: Geology, v. 39, p. 591–594, doi:10.1130/G31838.1.

Minjin, C., 2001, Notes to accompany the correlation of the Ordovician and Silurian rocks of Mongolia, *in* Minjin, C., and Tumenbayer, B., eds., The Guidebook, Mongolian Ordovician and Silurian Stratigraphy and Abstracts for the Joint Field Meeting of IGCP 410-IGCP 421 in Mongolia, Parts I–IV: Ulaanbaatar, Mongolia, p. 96–107.

Mulder, T., and Syvitski, J.P.M., 1995, Turbidity currents generated at river mouths during exceptional discharges to the world oceans: The Journal of Geology, v. 103, p. 285–299, doi:10.1086/629747.

Mulder, T., Syvitski, J.P.M., Migeon, S., Faugeres, J.C., and Savoye, B., 2003, Marine hyperpycnal flows: Initiation, behavior and related deposits. A review: Marine and Petroleum Geology, v. 20, p. 861–882, doi:10.1016/j.marpetgeo.2003.01.003.

Myrow, P.M., and Southard, J.B., 1991, Combined-flow model for vertical stratification sequences in shallow marine storm-dominated beds: Journal of Sedimentary Petrology, v. 61, p. 202–210.

Myrow, P.M., and Southard, J.B., 1996, Tempestite deposition: Journal of Sedimentary Research, v. 66, p. 875–887.

Myrow, P.M., Fischer, W., and Goodge, J.W., 2002, Wave-modified turbidites: Combined-flow shoreline and shelf deposits, Cambrian, Central Transantarctic Mountains:

Journal of Sedimentary Research, v. 72, p. 641–656, doi:10.1306/022102720641.

Myrow, P.M., Lukens, C., Lamb, M.P., Houck, K., and Strauss, J., 2008, Dynamics of a transgressive prodeltaic system: Implications for geography and climate with a Pennsylvanian intracratonic basin: Journal of Sedimentary Research, v. 78, p. 512–528, doi:10.2110/jsr.2008.061.

Myrow, P.M., Hughes, N.C., Goodge, J.W., Fanning, C.M., Williams, I.S., Peng, S., Bhargava, O.N., Parcha, S.K., and Pogue, K.R., 2010, Extraordinary transport and mixing of sediment across Himalayan central Gondwana during the Cambrian-Ordovician: Geological Society of America Bulletin, v. 122, p. 1660–1670, doi:10.1130/B30123.1.

Nittrouer, C.A., and Wright, L.D., 1994, Transport of particles across continental shelves: Reviews of Geophysics, v. 32, p. 85–113, doi:10.1029/93RG02603.

Ogg, J.G., Ogg, G., and Gradstein, F.M., 2008, The Concise Geologic Time scale: Cambridge, UK, Cambridge University Press, 150 p.

Ogston, A.S., and Sternberg, R.W., 1999, Sediment-transport events on the northern California continental shelf: Marine Geology, v. 154, p. 69–82, doi:10.1016/S0025-3227(98)00104-2.

Pattison, S.A.J., 2005, Storm-influenced prodelta turbidite complex in the lower Kenilworth Member at Hatch Mesa, Book Cliffs, Utah, U.S.A.: Implications for shallow marine facies models: Journal of Sedimentary Research, v. 75, p. 420–439, doi:10.2110/jsr.2005.033.

Plink-Björklund, P., and Steel, R.J., 2004, Initiation of turbidity currents: Outcrop evidence for Eocene hyperpycnal flow turbidites: Sedimentary Geology, v. 165, p. 29–52, doi:10.1016/j.sedgeo.2003.10.013.

Poller, U., Gladkochub, D., Donskaya, T., Mazukobzov, A., Sklyarov, E., and Todt, W., 2005, Multistage magmatic and metamorphic evolution in the Southern Siberian craton: Archean and Paleoproterozoic zircon ages revealed by SHRIMP and TIMS: Precambrian Research, v. 136, p. 353–368, doi:10.1016/j.precamres.2004.12.003.

Rojas-Agramonte, Y., Kröner, A., Demoux, A., Xia, X., Wang, A., Donskaya, T., Liu, D., and Sun, M., 2011, Detrital and xenocrystic zircon ages from Neoproterozoic to Palaeozoic arc terranes of Mongolia: Significance for the origin of crustal fragments in the Central Asian orogenic belt: Gondwana Research, v. 19, p. 751–763, doi:10.1016/j.gr.2010.10.004.

Rust, B.R., and Koster, E.H., 1984, Coarse alluvial deposits, *in* Walker, R.G., ed., Facies Models (2nd ed.): Toronto, Geoscience Canada, Reprint Series 1, p. 53–69.

Ruzhentsev, S.V., and Burashnikov, V.V., 1996, Tectonics of the western Mongolian Salairides: Geotectonics, v. 29, p. 379–394.

Sal'nikova, E.B., Kotov, A.B., and Belyatsky, B.B., 1997, U-Pb age of granitoids in the junction zone between the Olekma granite-greenstone and Aldan granulites-gneiss domains: Stratigraphy and Geological Correlation, v. 5, p. 3–12.

Şengör, A.M.C., Natal'in, B.A., and Burtman, V.S., 1993, Evolution of the Altaid tectonic collage and Paleozoic crustal growth in Eurasia: Nature, v. 364, p. 299–307, doi:10.1038/364299a0.

Southard, J.B., Lambie, J.M., Federico, D.C., Pile, H.T., and Weidman, C.R., 1990, Experiments on bed configurations in fine sands under bidirectional purely oscillatory flow, and the origin of hummocky cross-stratification: Journal of Sedimentary Petrology, v. 60, p. 1–17.

Squire, R.J., Campbell, I.H., Allen, C.M., and Wilson, C.L., 2006, Did the Transgondwanan Supermountain trigger the explosive radiation of animals on Earth?: Earth and Planetary Science Letters, v. 250, p. 116–133, doi:10.1016/j.epsl.2006.07.032.

Stacey, J.S., and Kramers, J.D., 1975, Approximation of terrestrial lead isotope evolution by a two-stage model: Earth and Planetary Science Letters, v. 26, p. 207–221, doi:10.1016/0012-821X(75)90088-6.

Stratford, M.C., and Aitchison, J.C., 1996, Devonian intra-oceanic arc rift sedimentation—Facies development in the Gamilaroi terrane, New England orogen, eastern Australia: Sedimentary Geology, v. 101, p. 173–192, doi:10.1016/0037-0738(95)00063-1.

Traykovski, P., Geyer, W.R., Irish, J.D., and Lynch, J.F., 2000, The role of wave induced density-driven fluid mud flows for cross-shelf transport on the Eel River continental shelf: Continental Shelf Research, v. 20, p. 2113–2140, doi:10.1016/S0278-4343(00)00071-6.

Trowbridge, J.H., and Kineke, G.C., 1994, Structure and dynamics of fluid muds on the Amazon continental shelf: Journal of Geophysical Research, v. 99, p. 865–874, doi:10.1029/93JC02860.

Van den Berg, J.H., Vangelder, A., and Masterbergen, D.R., 2002, The importance of breaching as a mechanism of subaqueous slope failure in fine sand: Sedimentology, v. 49, p. 81–95, doi:10.1046/j.1365-3091.2002.00433.x.

Wang, C., Weddige, K., and Minjin, C., 2005, Age revision of some Paleozoic strata of Mongolia based on conodonts: Journal of Asian Earth Sciences, v. 25, p. 759–771, doi:10.1016/j.jseaes.2004.07.008.

Warrick, J.A., and Milliman, J.D., 2003, Hyperpycnal sediment discharge from semiarid southern California rivers: Implications for coastal sediment budgets: Geology, v. 31, p. 781–784, doi:10.1130/G19671.1.

Windley, B.F., Alexeiev, D., Xiao, W., Kröner, A., and Badarch, G., 2007, Tectonic models for accretion of the Central Asian orogenic belt: Journal of the Geologic Society of London, v. 164, p. 31–47, doi:10.1144/0016-76492006-022.

Wong, K., Sun, M., Zhao, G., Yuan, C., and Xiao, W., 2010, Geochemical and geochronological studies of the Alegedayi ophiolitic complex and its implication for the evolution of the Chinese Altai: Gondwana Research, v. 18, p. 438–454, doi:10.1016/j.gr.2010.01.010.

Wright, L.D., and Friedrichs, C.T., 2006, Gravity-driven sediment transport on continental shelves: A status report: Continental Shelf Research, v. 26, p. 2092–2107, doi:10.1016/j.csr.2006.07.008.

Xiao, W., Han, C., Yuan, C., Sun, M., Lin, S., Chen, H., Li, Z., Li, J., and Sun, S., 2008, Middle Cambrian to Permian subduction-related accretionary orogenesis of Northern Xinjiang, NW China: Implications for the tectonic evolution of central Asia: Journal of Asian Earth Sciences, v. 32, p. 102–117, doi:10.1016/j.jseaes.2007.10.008.

Xiao, W., Huang, B., Han, C., Sun, S., and Li, J., 2010, A review of the western part of the Altaids: A key to understanding the architecture of accretionary orogens: Gondwana Research, v. 18, p. 253–273, doi:10.1016/j.gr.2010.01.007.

Xiao, W.J., Windley, B.F., Yuan, C., Sun, M., Han, C.M., Lin, S.F., Chen, H.L., Yan, Q.R., Liu, D.Y., Qin, K.Z., Li, J.L., and Sun, S., 2009a, Paleozoic multiple subduction-accretion processes of the southern Altaids: American Journal of Science, v. 309, p. 221–270, doi:10.2475/03.2009.02.

Xiao, W.J., Windley, B.F., Huang, B.C., Han, C.M., Yuan, C., Chen, H.L., Sun, M., Sun, S., and Li, J.L., 2009b, End-Permian to mid-Triassic termination of the accretionary processes of the Altaids: Implications for the geodynamic evolution, Phanerozoic continental growth, and metallogeny of Central Asia: International Journal of Earth Sciences, v. 98, p. 1189–1217, doi:10.1007/s00531-008-0407-z.

Yang, B., Dalrymple, R.W., and Chun, S., 2006, The significance of hummocky cross-stratification (HCS) wavelengths: Evidence from an open-coast tidal flat, South Korea: Journal of Sedimentary Research, v. 76, p. 2–8, doi:10.2110/jsr.2006.01.

Zorin, Y.A., Belichenko, V.G., Turutanov, F.K., Kozhenvnikov, V.M., Ruzhentsev, S.V., Dergunov, A.B., Filippova, I.B., Tornurtogoo, O., Arvisbaatar, N., Bayasgalan, T., Biambaa, C., and Khosbayar, P., 1993, The South Siberia-Central Mongolia transect: Tectonophysics, v. 225, p. 361–378, doi:10.1016/0040-1951(93)90305-4.

Science Editor: Christian Koeberl
Associate Editor: Peter A. Cawood

Manuscript Received 18 June 2012
Revised Manuscript Received 17 December 2012
Manuscript Accepted 19 December 2012

Printed in the USA